



**UNIVERSITA' POLITECNICA DELLE MARCHE**

**FACULTY OF ENGINEERING**

---

Master's Degree in **Biomedical Engineering**

**ROBOT-BASED MEASUREMENT OF COMFORT THROUGH THERMAL INFRARED  
IMAGING AND PHYSIOLOGICAL SIGNALS**

Supervisor:

**Prof. Eng. Gian Marco Revel**

Candidate:

**Vittoria Cipollone**

Co-supervisors:

**Ph.D Nicole Morresi**

**Prof. Eng. Sara Casaccia**

**A.Y. 2020 / 2021**



## **SUMMARY**

|  |           |
|--|-----------|
| <b>ABSTRACT .....</b>  | <b>1</b>  |
| <b>CHAPTER 1: INTRODUCTION .....</b>                                   | <b>2</b>  |
| 1.1 Background and motivations .....                                   | 2         |
| 1.2 Objectives .....   | 5         |
| 1.3 Related Work .....   | 6         |
| <b>CHAPTER 2: STATE OF ART .....</b>                                   | <b>8</b>  |
| 2.1 Thermal comfort .....  | 8         |
| 2.2 Thermal comfort and human physiology .....                         | 9         |
| 2.3 Thermal comfort models and its assessment .....                    | 11        |
| 2.3.1 The rational or heat-balance approach (PMV and PPD models) ..... | 12        |
| 2.3.2 Adaptive methods.....  | 15        |
| 2.3.3 Innovative methodologies for thermal comfort assessment .....    | 16        |
| 2.3.4 Robot-based measurement for thermal comfort assessment .....     | 18        |
| 2.4 Limitations of the state of art .....                              | 20        |
| <b>CHAPTER 3: MATERIALS AND METHODS .....</b>                          | <b>22</b> |
| 3.1 SENSORS AND DEVICES .....  | 23        |
| 3.1.1 Sensorized Robot (Misty II) .....                                | 24        |
| 3.1.2 Single-Board Computer.....                                       | 26        |
| 3.1.3 Smartwatch.....  | 27        |
| 3.1.4 Environmental sensor .....                                       | 28        |
| 3.1.5 Infrared sensor .....  | 29        |
| 3.2 MEASUREMENT SETUP .....  | 31        |
| 3.2.1 Measurement setup procedure .....                                | 32        |
| 3.2.2 Software integration .....                                       | 35        |
| 3.3 TESTS.....   | 37        |
| 3.3.1 Participants .....   | 41        |

|  |           |
|--|-----------|
| 3.4 DATA ANALYSIS.....                                 | 41        |
| 3.4.1 Measurement procedure and software dataflow..... | 42        |
| 3.4.2 Data processing .....                            | 46        |
| <b>CHAPTER 4: RESULTS .....</b>                        | <b>50</b> |
| 4.1 Feasibility of the robot-based method.....         | 50        |
| 4.1 Results of TSV prediction in post-processing ..... | 51        |
| <b>CHAPTER 5: DISCUSSION.....</b>                      | <b>53</b> |
| <b>CHAPTER 6: CONCLUSIONS .....</b>                    | <b>55</b> |
| <b>REFERENCES .....</b>                                | <b>56</b> |

# LIST OF FIGURES

|   |    |
|---|----|
| Figure 1. The ASHRAE seven-point scale [1]. It is possible to appreciate how each range quantifies the occupant's thermal sensation. ....   | 3  |
| Figure 2. Representation of GUARDIAN ecosystem. ....  | 7  |
| Figure 3. In this figure, it is possible to observe an intuitive representation of how PMV model works. Given the parameters shown on the left, the PMV formula can compute a number which represent the occupant's thermal sensation accordingly to the norm ASHRAE 55. .... | 12 |
| Figure 4. Relationship between PPD and PMV. ....  | 14 |
| Figure 5. Block scheme describing the workflow of the overall research. ....  | 23 |
| Figure 6. Misty II on-board sensors. ....   | 25 |
| Figure 7. Raspberry Pi 4 model B and its GPIO pins. ....  | 26 |
| Figure 8. Samsung Galaxy Watch. ....  | 27 |
| Figure 9. DHT11 and its pins. It is possible to appreciate that there are two kinds of DHT11 depending on the number of pinouts. ....   | 29 |
| Figure 10. (a) Lepton 3.5 and its Breakout Board v2.0. (b) The IR sensor inserted in its board. ....  | 30 |
| Figure 11. Visual representation of DHT11 connection with Raspberry Pi 4. ....  | 32 |
| Figure 12. Pins configuration of the Breakout Board v2.0. ....  | 33 |
| Figure 13. The Lepton module setup developed in the current work. ....  | 33 |
| Figure 14. The application “HeartRate_NM2” developed in the current work. ....  | 34 |
| Figure 15. Extract of the JavaScript code of the smartwatch application. ....   | 35 |
| Figure 16. Extract of the Python code for “Get_env_params” function implementation. ....  | 35 |
| Figure 17. Extract of the “get_temp” Python function implemented for the current work. ....   | 36 |
| Figure 18. Three examples of IR frames captured by Lepton 3.5. ....   | 36 |
| Figure 19. Extract of Python code where several functions have been implemented in order to exploits Samsung Galaxy Watch collected data. ....  | 37 |
| Figure 20. Planimetry of the room used for the experimental procedure. It is also possible to appreciate how some devices have been placed inside the room. ....  | 38 |
| Figure 21. Pictures of how the indoor space has been organized during the trials. In the second image (b) it is possible to see how and where the Lepton module has been attached (red circle). ....  | 38 |
| Figure 22. (a) Microclimatic station; (b) ultrparametric belt; (c) temperature sensor iButton; (d) thermal camera. ....   | 39 |
| Figure 23. Trend of the environmental temperature reached during the three trials. ....   | 40 |
| Figure 24. Flowchart of the logic at the base of the Python code for real-time TSV prediction. ....   | 42 |
| Figure 25. Extract of “face_detect” function used as first step of the whole workflow. ....   | 43 |
| Figure 26. Python code extract of the first part of data acquisition phase. ....  | 43 |
| Figure 27. Two examples of face detection output performed by Misty II. The rectangle identifies the subjects in front of the robot. ....   | 44 |
| Figure 28. Python code extract where the ML algorithm is imported for the TSV prediction. ....  | 45 |
| Figure 29. The three expressions that can be visualized on Misty II display according to the predicted TSV value. (a) Joy expression for thermal comfort case; (b) Terror expression for cold discomfort case; (c) Fear expression for hot discomfort case. ....              | 45 |
| Figure 30. Block scheme that resumes all the passages of the second part of data analysis. ....   | 46 |

Figure 31. (a) HRV signal of subject 1 during the cold trial. (b) the HR signal of subject 1 during the cold trial. In both (a) and (b) the blue trace is the original signal, while the orange one is the processed one. ....47

Figure 32. Plots of the TSV prediction output against the TSV acquired during the three days of tests from the 10 participants. (a) Plot with Random Forest prediction output. (b) Plot with Naïve Bayes prediction output. (c) Plot with K-Nearest Neighbor prediction output. (d) Plot with Decision Tree prediction output. (e) Plot with Adaboost prediction output. (f) Plot with Bagged Tree prediction output. (g) Plot with Support Vector Machine prediction output.....51

## LIST OF TABLES

|   |    |
|---|----|
| Table 1. Technical information of the smartwatch employed in this study (Samsung Galaxy Watch)..... | 28 |
| Table 2. Technical specifications of DHT11. ....  | 29 |
| Table 3. Technical specifications of Flir Lepton 3.5. ....  | 30 |
| Table 4. Devices integrated with Raspberry Pi 4 and Misty II. ....                                  | 31 |
| Table 5. DHT11 pins and the correspondent Raspberry GPIO pins. ....                                 | 32 |
| Table 6. Pins configuration for Lepton 3.5 and Raspberry Pi 4 connection. ....                      | 34 |
| Table 7. Anthropometric features of the participants. ....  | 41 |
| Table 8. List of the Machine Learning algorithms used in this study.....                            | 48 |
| Table 9. Input dataset for the Machine Learning algorithms used in this study. ....                 | 48 |
| Table 9. Pros and Cons of the methodology developed in this master thesis. ....                     | 50 |
| Table 10. Accuracies of the employed ML algorithms.....   | 52 |

## LIST OF SYMBOLS

| Symbol | Description                              |
|--------|--|
| PMV    | Predicted Mean Vote [-]                  |
| PPD    | Predicted Percentage of Dissatisfied [%] |
| EDA    | Electrodermal activity [ $\mu$ S]        |
| HR     | Heart rate [bpm]                         |
| HRV    | Heart Rate Variability [ms]              |
| $t_a$  | Air Temperature [ $^{\circ}$ C]          |
| $v_a$  | Air velocity [m/s]                       |
| RH     | Relative Humidity [%]                    |

---

## LIST OF ABBREVIATIONS

| Abbreviation | Description  |
|--------------|--|
| AI           | Artificial Intelligence  |
| ML           | Machine Learning   |
| TSV          | Thermal Sensation Vote   |
| HVAC         | Heating, Ventilation and Air-Conditioning                                  |
| ASHRAE       | American Society of Heating, Refrigerating, and Air-Conditioning Engineers |
| ISO          | International Organization of Standardization                              |
| TSI          | Thermal Sensation Index  |
| PCM          | Personal Comfort Model   |
| ECG          | Electrocardiogram  |
| EEG          | Electroencephalogram   |
| AAL          | Active and Assisted Living   |
| IEQ          | Indoor Environmental Quality   |
| IAQ          | Indoor Air Quality   |
| ANS          | Autonomous Nervous System  |

---

# ABSTRACT

This master thesis shows the outcome of an innovative measurement methodology for the assessment of thermal comfort through a robotic structure. The thermal sensation vote (TSV) is measured by a social robot that acquires indoor environmental parameters (air temperature and relative humidity) and physiological parameters such as heart rate variability and skin temperature. Low-cost and minimally invasive sensors (i.e. smartwatch, infrared sensor) were integrated into the robot and the proposed solution has been tested on 10 participants during a three days measurement campaign.

The development of this method aims at overcoming the lack of a personalized and robot-based technique for thermal comfort measurement. Indeed, the traditional methodology is based on the computation of Predicted Mean Vote (PMV) and Percentage of People Dissatisfied (PPD) which give an overall estimation of thermal comfort in a group of subjects not considering thermal differences among individuals. Further studies have introduced adaptive methods which assess human thermal sensation starting from both physiological signals and environmental parameters. However, the tools and devices used in this case are invasive, expensive and they do not guarantee an accurate measurement. Hence, wearable sensors and infrared technologies have been introduced. Moreover, the increasing relevance of the Internet of Things (IoT) and Artificial Intelligence (AI) led scientific research to thermal comfort assessment procedures with Machine Learning (ML) and robotic systems. Nevertheless, they are still not user-centered methodologies.

Based on these considerations, the proposed robot-based method succeeds in measuring thermal comfort expressed as TSV via ML algorithms. The used dataset is composed of physiological and environmental parameters acquired by the integrated robotic structure. The employed ML algorithms have reached different predictive accuracies and among them, the Random Forest classifier and the Naïve Bayes provided the highest one.

Hence, the present study demonstrates the feasibility of the robot-based methodology in the scenario of thermal comfort assessment. Nevertheless, this master thesis shows some limitations that mainly concern the quality of the collected data and the real-life context application. Future studies may enlarge the input dataset of ML algorithms by developing longer experimental protocols. Moreover, an automatization procedure can be developed to obtain a methodology tailored to people's everyday lives.

# CHAPTER 1: INTRODUCTION

## *1.1 Background and motivations*

The subjectivity of the thermal sensation experienced by humans in response to the thermal environment is a topic of interest among the scientific community since thermal comfort deeply affects human health. It has been widely demonstrated that in a group of subjects there will be people who differently perceive the temperature of the environment even though the occupied room is characterized by the same thermal conditions. This phenomenon occurs since behavioral and physiological factors deeply influence the human thermal sensation: there will be always a person who is thermally comfortable in the same room where another subject feels uncomfortable.

Hence, since people spend the 80% of their time in indoor environments and given the impact of the thermal conditions on people's health, several norms and indicators have been employed to guarantee occupants' well-being in everyday facilities. Indeed, recent studies have supplied techniques which consider the human being as central component of the whole system: the subject is an active element of the indoor space and the thermal sensation is the main target since it would influence the daily productivity, mood and health.

However, optimum thermal comfort concerns also building energy efficiency. Thus, the development of an effective methodology for thermal comfort assessment hides a dual purpose:

- The possibility to obtain optimal indoor conditions for health and productivity reducing thermal stress;
- The improvement of building efficiency given the high percentage of energy consumption that structures produce in order to manage Heating, Ventilation and Air-Conditioning (HVAC) systems [1].

Nevertheless, people still experience thermal discomfort despite the significant energy consumption. Thus, there is an imbalance between the energy spent to possibly guarantee thermal comfort and the actual energy demand for a thermally comfortable indoor space.

Consequently, thermal comfort has been analyzed and studied in multiple engineering fields with the aim of finding an objective interpretation that can be exploited in the HVAC control systems. However, the subjectivity of thermal sensation makes its assessment still challenging. In fact, lots of factors and parameters should be considered to achieve a realistic interpretation of human thermal sensation. For these reasons, in literature it is possible to find a heterogenous group of methodologies which approach this issue in different ways.

The current guidelines for a proper thermal comfort assessment are provided by norms of the American Society of Heating, Refrigerating and Air-Conditioning Engineers (ASHRAE) such as ASHRAE 55 [2] and ISO 7730 [3] where thermal comfort evaluation is related to the thermal sensation vote (TSV) and thermal sensation index (TSI). They are both based on the ASHRAE seven-point thermal sensation scale (Figure 1) [1] which paved the way to prediction methods such as the Predicted Mean Vote (PMV) model and Predicted Percentage of Dissatisfied (PPD) proposed by Fanger et al. [4]. Their main disadvantage is the impracticability in real-life situations due to the absence of parameters related to the human body response to thermal changes [5].

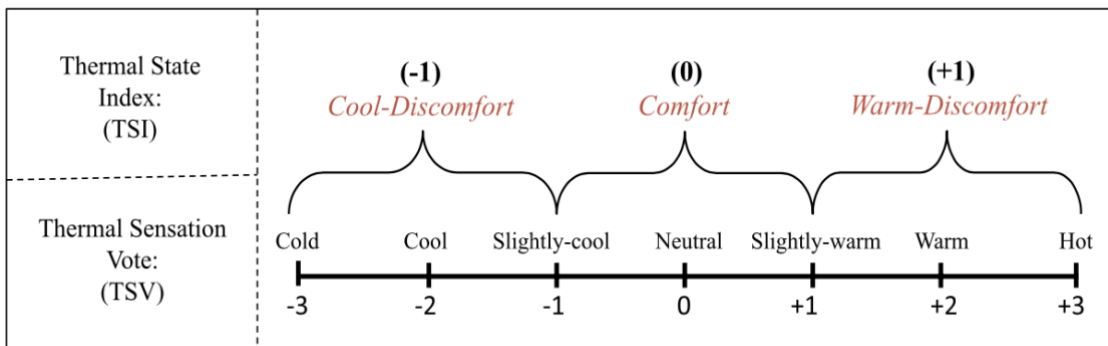


**Figure 1.** The ASHRAE seven-point scale [1]. It is possible to appreciate how each range quantifies the occupant's thermal sensation.

Given that, further studies have introduced more personal factors such as physiological parameters to obtain a more realistic and customized estimation of thermal sensation. Thus, Personal Comfort Models (PCM) have been proposed as alternative methods for a personalized thermal comfort prediction. PCMs exploited human physiology responses to temperature variations by detecting physiological signals through specific sensors. Electrocardiogram (ECG), Electroencephalograph (EEG), devices for Electrodermal Activity (EDA) [1] have been widely used in this scientific field given their high accuracy and sensitivity.

Indeed, the combination of physiological parameters (i.e., Heart Rate (HR), Heart Rate Variability (HRV), skin temperature, brain activity) with environmental factors (Indoor air temperature ( $t_a$ ), relative humidity (RH), air velocity ( $v_a$ ) etc.) represented the best input data for a more reliable thermal comfort measurement. Nevertheless, some studies have defined the previously mentioned sensing methods as invasive procedures since the sensors are attached to the user for a long period of time, leading to limited activity during the assessment and uncomfortable sensation [6].

The introduction wearable technologies and infrared sensors is becoming preferable for thermal comfort assessment due to the reduction in invasiveness of the devices and the increasing accuracy that they provide. In addition, the development of Artificial Intelligence (AI), Machine Learning (ML) and Deep Learning algorithms led the scientific community to focus on new techniques which exploit the traditional thermal comfort parameters as input data. These innovative approaches outperform the traditional ones reaching more reliable percentages of accuracy [7], [8]. Furthermore, recent studies have combined the just mentioned methodologies with the introduction of robotic systems. These last ones are characterized by several hardware components such as microcontrollers, sensors and RGB cameras. The development of this idea has been driven by the need of an automated device (the robot) which may be possibly applied in real-life use cases such as a working environment. Finally, the increasing reliability of robots have led to their introduction in the social environment as helper and companions for specific categories of people such as elderly people or caregivers. Hence, the figure of social robot was born in order to provide aid and support in everyday life situations. Misty II by Misty Robotics is one of the most recent robotic structure exploited for this purpose. It is a multi-sensor robot that can efficiently recognize people, interact with them and it can be also handled by developers whether they want to add or modify some of Misty's skills.

However, at present the proposed robotic devices aim at measuring thermal comfort by processing only environmental parameters without considering user-related factors (physiological signals). Furthermore, robotic companions like Misty II are still not exploited in this engineering field.

Thus, a methodology that objectively quantify thermal comfort giving higher importance to the detection of bio-signals is still not present in literature. Moreover, occupants'

thermal sensation is a dynamic phenomenon that continuously changes together with people's thermal preference due to the thermal heterogeneity of the environment. In fact, the indoor thermal state can modify based on user-related factors (the occupants change the thermal condition of the room acting on the HVAC system) and the outdoor thermal conditions. Thus, the variability of environmental thermal state and of the subject thermal perception make thermal comfort assessment still an open challenge and it also stresses the pivotal need of a user-centered procedure.

## ***1.2 Objectives***

The continuous technological development led to the introduction of innovative methods and instrumentations in the field of thermal comfort assessment. Given the increasing relevance that wearable technologies and ML have gained in the last decades, literature reports several studies that have based their experiments on them [1], [9], [8]. Furthermore, the technological progress allowed some researchers to attempt the development of thermal comfort assessment procedures based on robotic structures. In particular, some studies have integrated all the sensors that are typically used for thermal comfort assessment in a robotic system in order to obtain a more automatized measurement [10], [11].

However, it has not been proposed a methodology that quantify thermal comfort starting from the detection of both environmental and physiological parameters through the employment of robotic structures and the computation of ML algorithms. Furthermore, in literature it is still missing a procedure that considers the human being as the main cause that drives the need of a thermal comfort assessment process. Hence, it is needed a method that measures thermal comfort in relation to what are the user needs in order to prevent and improve his or her well-being in certain indoor spaces.

Thermal comfort assessment is still an open issue despite the technological innovations widely used in this scientific scenario. For these reasons, in the current work, a deep literature analysis has been performed to understand which are the procedures that at present researchers are using in this engineering field so that an alternative methodology for the thermal comfort assessment can be found. Specifically, it will be designed a system which includes the social robot Misty II that interfaces directly the subject providing him or her an evaluation of the thermal comfort. This system will be built

considering a specific set of sensors for the detection of both physiological signals and environmental parameters. In this study all the knowledge provided by the past research will be exploited in order to propose a technique for thermal comfort assessment that can overcome their limitation and that gives to the human being and human health a central role.

In conclusion, it is possible to sum up the main goals of this master thesis in:

- Detecting physiological parameters such as HRV and skin temperature through wearable and infrared technology and also acquiring environmental parameters such as  $t_a$  and RH;
- Proposing a methodology that measures thermal comfort in real-time through the implementation of ML algorithms;
- Computing the accuracies of the employed ML algorithms to verify which is the most reliable for thermal comfort assessment;
- Involving a mobile robot that directly interfaces the user and gives an objective evaluation of the occupants' thermal state.

### ***1.3 Related Work***

The current master thesis is part of a larger project called GUARDIAN which is included in the AAL (Active and Assisted Living) program started on the 1<sup>st</sup> of January 2020 ([GUARDIAN project](#) , [AAL program](#) ). This European research project involves 10 participants that come from Italy, Netherlands, and Switzerland. Its goal is to develop a care robot (the Guardian Robot) that supports seniors and caregivers. Indeed, it provides an innovative approach to help caregivers and informal carers through a social robot that:

- Gives information to the caregiver about the elderly people's health through human-robot dialogue and sensing;
- Aids elderly people during their everyday life activities through reminders.

Moreover, another aspect that the GUARDIAN project tries to demonstrate is the advantage of introducing a social robot in long-term care scenarios in terms of cost-effectiveness and cost reductions.

GUARDIAN is a platform that consists of a social robot in the home of the elderly that is connected to caregiver apps through the GUARDIAN cloud. The whole GUARDIAN ecosystem can be appreciated in Figure 2. The social robot serves both as a companion of the elderly and as the ‘eyes, ears and a communication channel’ for the caregiver. It senses the overall well-being of frail people and provides feedback to the formal and informal caregivers reducing stress and care burden.

Based on that, the current master thesis gives its contribution to this European research project since it provides a non-invasive and personalized methodology for thermal comfort assessment through the usage of the social robot involved in the GUARDIAN project (Misty II). Indeed, thermal discomfort in indoor spaces can provoke severe consequences on human health and in particular on susceptible subjects such as elderly people. For this reason, the present work proposes a measurement technique for thermal comfort quantification which tries to be as user-friendly as possible and to improve the quality of people’s everyday life.

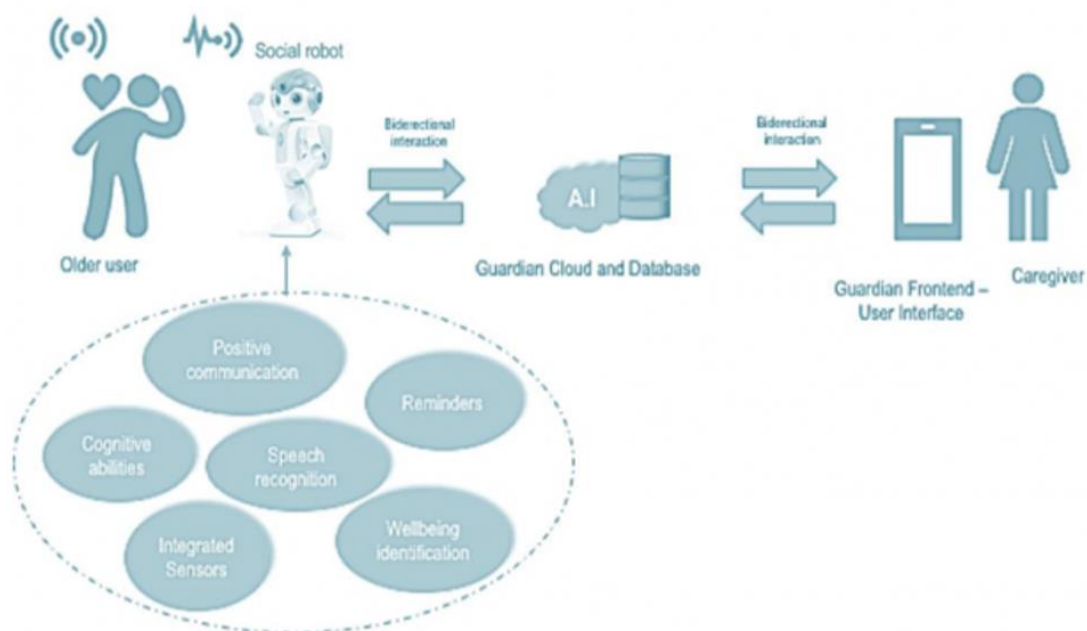


**Figure 2.** Representation of GUARDIAN ecosystem.

## CHAPTER 2: STATE OF ART

### *2.1 Thermal comfort*

The American Society of Heating, Refrigerating and Air-Conditioning Engineers (ASHRAE) officially defines thermal comfort as “the condition of mind which expresses satisfaction with the thermal environment and is assessed by subjective evaluation” [2], [12], [7]. Thus, comfort is not a state condition, but rather a state of mind. Subjectivity is the key element that modifies thermal perception from person to person and make thermal comfort a cognitive process that involves different kind of inputs such as physical, psychological, and physiological factors [13]. Indeed, thermal sensations are different among a group of individuals even though they occupy the same environment. People staying in similar spaces and subjected to the same thermal condition will experience very different thermal sensation due to the large number of factors that affect it. Consequently, it is not possible to find a methodology that is common for any subject, but it is convenient to find a technique that gives importance to physiological signals to achieve an accurate estimation of human thermal sensation.

Therefore, one of the aspect that should be taken into consideration when developing a thermal comfort study is how people’s physiology, wellbeing and productivity are affected by environmental, personal, and behavioral factors [14]. The first kind includes all the parameters that physically characterize an indoor environment (i.e.,  $t_a$ , RH,  $v_a$  and  $t_r$ ). Personal factors instead are related to the physiological features of an individual (e.g., age, gender, Body Mass Index), while behavioral factors include the activities that the subject usually performs and the kind of clothes the individual is wearing [14], [15]. Indeed, metabolic rate and clothing insulation are the most traditional aspects that are assessed to quantify thermal comfort.

Given that, indoor thermal comfort has become a topic of interest in many engineering fields due to its impact on people wellbeing and on building energy consumption. Indeed, in order to establish and maintain the most optimal thermal conditions for occupant, buildings efficiency is compromised due to the high energy consumption for a proper regulation of the HVAC systems [1], [8]. Hence, the crucial need to reduce the economic

and environmental cost of energy consumption enriched the scientific literature with lots of research concerning thermal comfort from the sustainability point of view.

Instead, the deep influence of thermal comfort on people well-being and health, led the scientific community to find a reliable methodology for thermal sensation prediction starting from physiological factors in order to improve people daily routine and avoid precarious health conditions during simple everyday activities. It is also true that health and thermal comfort are strictly related to the indoor environmental quality (IEQ) which is a more general parameter that in turn depends on several factors such as: indoor air quality (IAQ), thermal comfort, lighting environment, and acoustic comfort. As people spend 90% of their time indoors, having a good IEQ is particularly important since a long-term exposure to low-quality air can cause chronic conditions such as cardiovascular and respiratory diseases [1], [16], [14], [17].

Hence, thermal discomfort can be a real threat for occupants and it can be particularly critical in case of susceptible subjects [18], [19]. For instance, elderly people's health can be compromised during their daily activity due to a too cold or too hot environment. In fact, heart-related complications or heart failures can be triggered by too warm environments, while too cold thermal conditions lead to a decrease of the body core temperature which provokes drowsiness, lethargy and even death. The cause of these phenomena is the defective adaptive mechanisms of susceptible subjects that fail in restoring the internal homeostasis of their physiological system.

In conclusion, the design of a thermal comfort prediction model can give a remarkable contribution to the improvement of both occupants' health during their daily routine and the building energy-efficiency through strategic ambient-control systems.

## ***2.2 Thermal comfort and human physiology***

From a physiological point of view, the human body can be seen as a thermal machine which is able to exchange energy with the external environment according to specific chemical processes that build the human metabolism [15]. Specifically, the general law that must rule on the human body is that the rate of heat produced by the body must be equal to the rate of heat loss of the body [2]. This principle is satisfied thanks to the thermoregulation processes: indeed, when external factors (e.g., temperature or humidity

variation) or internal factors provokes thermal stress (i.e., feeling too hot or too cold), the human body reacts, and the thermoregulation system is triggered. It adjusts heat dissipation by modifying the blood flow via arterioles and veins (causing vasodilatation or vasoconstriction phenomena) in order to restore the physiological homeostasis [20].

Hence, human health can be weakened in case of prolonged thermal discomfort, mostly when occupants are vulnerable subjects such as elderly people whose adaptive mechanisms are surely less reactive than younger people's. Indeed, as mentioned before a prolonged exposure to a too warm or a too cold environment can lead to heart complications, respiratory problems and even death [5]. Thus, it is clear how thermal comfort assessment is crucial for a pleasant and even safe experience inside certain facilities.

As a result, several studies have suggested the feasibility of using physiological signals such as skin temperature, HR and its variability (HRV) and brain activity to assess occupants' thermal comfort.

For instance, in reference [21] the thermal sensations of subjects have been measured with respect to their mean skin temperature applying three environmental conditions (slightly cool, neutral, warm) and using linear regression models. In this way, the thermoregulation process of vasodilatation and vasoconstriction have been objectively linked to the thermal sensation of the occupants.

Given that thermal comfort is officially defined as a state of mind [2], several studies have recorded brain activities via EEG while the environment thermally changed [22]. It has been observed how the spectral power of the EEG signals changes based on the thermal sensation of the subject. Specifically, Lim et al. [23] have proposed two effective indexes for thermal sensation assessment starting from brain waves recordings.

Researchers have also investigated heart rate and its effectiveness for thermal comfort measurement since cardiac activity is strictly influenced by the subject's metabolic level and work intensity, which are two factors that modify how the occupant thermally perceives the environment [24]. Moreover, HRV reflects the activity of the Autonomous Nervous System (ANS) which is deeply involved in thermoregulatory processes triggered in case of thermal discomfort [25]. Thus, HRV observation during different thermal conditions can be another method to physiologically measure thermal comfort. Several

studies have performed a HRV spectral analysis through ECG signals in order to detect possible abnormalities caused by environmental temperature variations [22].

Despite these physiological-based techniques have proved the presence of several physiological responses correlated with thermal comfort and discomfort, all the sensors and instrumentations that are traditionally used in this research field may be a real issue. In fact, some studies consider them as invasive tools since they are directly in contact with the subjects' bodies, requiring their continuous presence for a long period of time. Moreover, the accuracy of their sensing performance deeply depends on how sensors are placed on the subjects' body and on the level of activity and movements performed by the subjects [20].

However, the continuous development of new technologies has guided researchers to analyze and employ innovative sensors which can assess physiological parameters without being an obstacle for subjects. Among them, wearable sensors such as smartwatches or smart bands and infrared sensors or thermal cameras have become a topic of interest in the thermal comfort assessment scenario.

### ***2.3 Thermal comfort models and its assessment***

Several proposals for a thermal comfort assessment methodology have been developed in the last few decades [26] and most of them have been standardized (ASHRAE Standard 55, ISO 7033, EN 15251) and employed given the crucial role that thermal sensation has on occupants' health and work productivity. Moreover, the frequency with which lots of people spend the main part of their daily routine inside a building has led different scientists to study thermically comfortable environments in order to improve occupants' stay in everyday life facilities [27]. Thus, thermal comfort assessment is the turning point procedure to quantify, predict and then improve the human satisfaction and health during their daily routine.

Therefore, it is pivotal to describe the methods that have conducted several researchers to the development of models for thermal comfort measurement. At present, two different approaches for the quantification of thermal comfort are used: the rational or heat-balance approach and the adaptive approach [13]. The rational approach uses data from steady-

state experiments based on climatic chamber employment, while the adaptive approach uses data from field studies of people in buildings.

### 2.3.1 The rational or heat-balance approach (PMV and PPD models)

The rational or heat balance approach includes all those models that are suitable for humans involved in near-sedentary activity and steady-state conditions. Thermal comfort is generally assessed among a group of occupants that performs everyday simple activity (studying, working, using a computer, speaking) while the environment is subjected to temperature variations. Indeed, climatic chambers are usually employed in order to verify which are the environmental conditions that provoke discomfort on occupants during sedentary situations.

These concepts are the basis for one of the most widespread methods used for thermal comfort assessment: the Predicted Mean Vote (PMV) model developed by Fanger et al. in the late 1960s.

The PMV index predicts the mean response of a large group of people according to the standard ASHRAE seven-point scale of thermal sensation (Fig.1). In fact, according to Franger’s research, subjects should be exposed to a climate chamber while giving their feedback in terms of thermal sensation following the seven-point scale mentioned before. Furthermore, PMV computation is based on a combination of physical and personal parameters. Indeed,  $T_a$ , air velocity, mean radiant temperature, RH, clothing insulation and metabolism had a crucial role in the PMV method evolution [4].

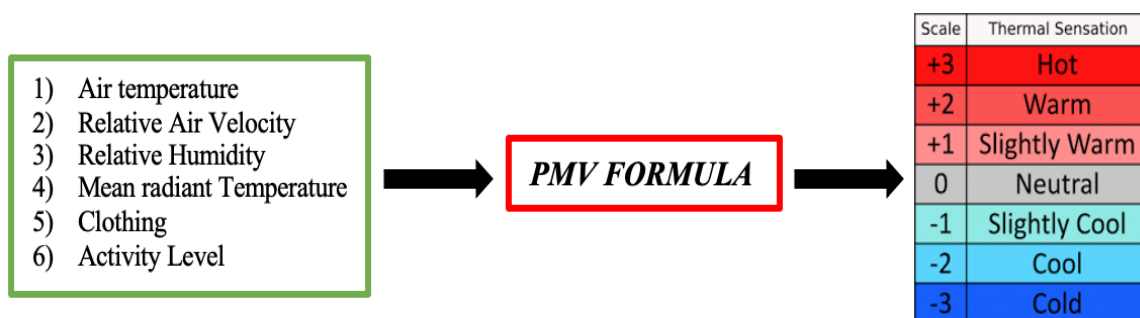


**Figure 3.** In this figure, it is possible to observe an intuitive representation of how PMV model works. Given the parameters shown on the left, the PMV formula can compute a number which represent the occupant's thermal sensation accordingly to the norm ASHRAE 55.

From a more practical point of view, PMV is obtained by considering the following equation:

$$PMV = (0.028 + 0.030 e^{(-0.036)})L = \alpha L \quad (1)$$

where  $\alpha$  is the sensitivity coefficient, while  $L$  is the thermal load on the body. Specifically,  $L$  represents the imbalance between the actual heat flow from a human body in a certain environment and the heat flow required for thermal comfort at a specified activity. Hence, it is the difference between the internal heat production and the heat loss to the environment for an occupant that is possibly comfortable [13], [4], [28]. Mathematically speaking,  $L$  can be computed with the following equation, that is the heat balance equation:

$$L = M - W - (C_{sk} + R + E_{sk}) + (C_{res} + E_{res}) \quad (2)$$

Where  $M$  is the metabolic energy,  $W$  is the accomplished work,  $C_{sk}$  is the convective heat flow of the skin (sk),  $R$  is the radiant one and  $E_{sk}$  is the evaporative heat flow of the skin (sk). As regards  $C_{res}$  and  $E_{res}$  they are respectively the respiratory (res) convective heat flow and the respiratory (res) evaporative one. Consequently, it is possible to define the PMV model as a heat balance model since it combines the theories of heat balance and the physiology of thermoregulatory system to determine a range of comfort temperatures. Indeed, thermal balance is reached when the internal heat production of the body is equal to the loss of heat given to the environment and when this balance is absent, the subject is not thermally comfortable. This phenomenon triggers the thermoregulatory system that acts to restore the physiological homeostasis by modifying skin temperature and by triggering sweat secretion [13], [3]. Fanger's studies lead to another index called Predicted Percentage of Dissatisfied (PPD) which gives the percentage of people predicted to experience local discomfort [29]. Starting from the seven-point scale of thermal sensation, it has been postulated that people who responded  $\pm 2$  and  $\pm 3$  are declared uncomfortable [13]. This percentage strictly depends on PMV as shown in the following equation:

$$PPD = 100 - 95 e^{[-(0.03350 PMV^4 + 0.2179 PMV^2)]} \quad (3)$$

Specifically, PPD ranges from 5% to 100% depending on the PMV value as reported in table 1 [30], [13].

**Table 1.** Comparison between PPD values and PMV ranges. In reference [30], they have been related to three comfort types.

| <i>Comfort</i> | <i>PPD</i> | <i>Range of PMV</i> |
|----------------|------------|---------------------|
| 1              | <6         | -0.2<PMV<0.2        |
| 2              | <10        | -0.5<PMV<0.5        |
| 3              | <15        | -0.7<PMV<0.7        |

Moreover, Eq. 3 reveals a perfect symmetry with respect to  $PMV = 0$ , that is thermal neutrality. It can be observed from Fig. 4 [31] that when the PMV index is 0, there are still some cases of thermal dissatisfaction, although all subjects are dressed in a similar way and the level of activity is the same. This is due to some differences of approach in the evaluation of thermal comfort from one person to another. Hence, thermal neutrality for different people is achieved at not identical environmental parameters. At  $PMV = 0$  it will exist a rate of dissatisfied equal to 5% [13], [28].

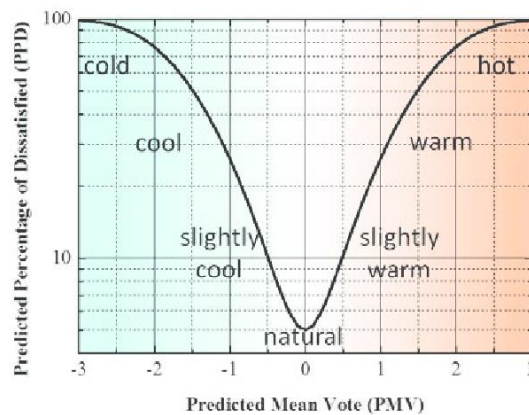


**Figure 4.** Relationship between PPD and PMV.

Given that, these models are commonly supported by surveys and questionnaires that occupants should fill when thermal comfort measurement occurs. In this way, it is possible to establish a comparison between the predicted thermal sensation and the actual thermal feeling that the subjects are perceiving. According to that, it has been proved that PMV model underestimate the real thermal sensation of people [32]. Moreover, PMV approach is characterized by other limitations mainly related to its application in real life situations [5]. Indeed, in the real-world setting the computation of the parameters used in

the PMV model is difficult and it leads to a low accuracy due to the dynamic nature of the metabolic rate and the clothing insulation that are not constant in time. Another limitation of the PMV model is that it derives from a study based on a strictly controlled climate chamber where the thermal environment is static. Thus, it is completely different from the real-life situations where temperature gradients are very common phenomena. Moreover, PMV only describes the overall thermal sensation of multiple occupants in a shared thermal environment since it predicts the average thermal sensation vote of a large group of people without considering the individual thermal comfort [33].

### **2.3.2 Adaptive methods**

Given the issues related to the traditional PPD and PMV methods, in recent years thermal comfort researches have been focused on to the concept of adaptation, i.e. the gradual decrease of the human response to repeated environmental stimulation [34]. Adaptive approach analyzes the acceptability of the environment from a thermal point of view, which strongly depends on the context, the behavior of occupants and their expectations [13]. The basic principle of this approach is how people are perceived: in fact, they are not passive receivers, but they are active participant in the dynamic equilibrium of the thermal environment. Furthermore, according to the adaptive hypothesis, contextual factors and past thermal history modify the occupant's thermal expectations and preferences [34]. This means that people who are used to cool environments will be thermally neutral in a situation where, instead, people coming from warmer environments feel uncomfortable. Hence, the evaluation of thermal comfort should be performed considering the individual thermal sensation and not the mean thermal sensation of large group of occupants.

The adaptive approach linearly relates the indoor air temperature with the outdoor one and it can be used for the evaluation of thermal comfort in free-running building and with people without a clothing regime. Hence, this method does not exploit the traditional factors proposed by Fanger since thermal neutrality not always coincide with the preferred thermal sensation of the occupants [34]. In fact, if on one hand Fanger has based his studies on a large group of occupants without considering how the individual would perceive thermal comfort, on the other hand the heterogeneity of thermal sensation from subject to subject is crucial to obtain a more adequate and realistic thermal comfort assessment.

The adaptive approach refers to statistical studies conducted in naturally ventilated buildings which include occupants in the control loop of the HVAC system, considering the interaction that in real life situation occurs between the subject and the environment. Despite the importance of the single subject in this model, physiological parameters are not fully exploited for a more accurate and personal thermal comfort evaluation. Thus, new scientific studies have introduced physiology in terms of physiological signals and parameters in order to obtain a more reliable and personalized evaluation of thermal comfort. Moreover, new techniques based on ML and AI have been developed with the aim of automating the measurement and improving the measurement accuracy.

### **2.3.3 Innovative methodologies for thermal comfort assessment**

With the increasing relevance of the Internet of Things (IoT), ML and AI applications, numerous scientific researches have proposed methods able to model individual comfort requirements based on the real-time acquisition of physiological and environmental parameters through specific sensors [8], [24]. In particular, the development of personalized comfort models relies on the combination of specific sets of data collected with environmental sensors, IR sensors, wearable devices or a combination of them [8]. The first category (environmental sensors) is used to monitor the physical parameters that have been always included in this kind of scientific field. Thus,  $t_a$ ,  $RH$ ,  $v_a$  and other common parameters are some of the variables that are detected using these tools. The turning point of these modern and innovative approaches is the introduction of infrared (IR) sensors and wearable devices such as smartwatches, since they acquire physiological information strictly related to the user, that capture the peculiarities among different humans. In this way, it is possible to continuously record human bio-signals such as HR and skin temperature whose variability underlines the influence of the environment on the occupants' health [7]. Moreover, the usage of wearable sensors represents the solution to the invasiveness problem. In fact, physiological data are acquired without wired sensors such as the ECG electrodes gaining the same accurate result without annoying the occupant.

For instance, in the study conducted by Ricardo et al. [35], the IR sensor FLIR Lepton 2.5 has been used to monitor subjects' attention through face temperature detection over time. Specifically, the Lepton module has been integrated into the single board computer

Raspberry Pi 3 and authors succeeded in detecting subjects' faces and computing face temperatures through ML algorithms.

In reference [36], the aim was the extraction of facial landmarks for face temperature assessment using both RGB cameras and IR sensors. Specifically, it has been demonstrated that the use of both these types of devices enhances the accuracy and reliability of the measurement, improving also the successive thermal comfort prediction. For their purpose, a 60x80 Flir Lepton camera module has been exploited given its low cost and reliability ( $\pm 5^{\circ}\text{C}$  temperature accuracy,  $0.1^{\circ}\text{C}$  temperature resolution). Furthermore, the ML algorithm Haar-Cascade has been used from a computational point of view to achieve the main goal of the study.

The emerging interest in ML algorithms application led scientific community to employ them and forecast thermal sensation directly from a pattern of heterogeneous data collected by the above-mentioned sensors [37]. Specifically, Random Forest (RF), Artificial Neural Network (ANN), Decision Trees (DT) and Support Vector Machine (SVM) are the most common procedures in the thermal comfort scenario with a predictive accuracy that ranges from 75 % to 95% [8].

For instance, Da Li et. Al [7] proposed a non-intrusive method that predicts thermal comfort with an accuracy of 85% and it is based on the detection of facial skin temperature through the usage of low-cost thermal cameras (Flir Lepton 2.5 radiometric thermal camera) and computer vision techniques (e.g., Haar Cascade object detection, Random Forest Classifier).

Chauduri et al. [1] designed the enhanced Predicted Thermal State (ePTS) method which exploits physiological parameters such as pulse rate and ST sensed through wearable technology in order to predict thermal sensation via SVM classifier. This approach outperforms the traditional models since it achieves an accuracy of 97% when physiological parameters are added to the most traditional ones (environmental parameters). Moreover, the same authors conducted a study [16] where two new approaches are developed based on inputs such as ST, pulse rate, oxygen saturation and blood pressure. They are both based on ML procedures: indeed, the first one uses a Convolutional Neural Network (CNN) that predicts thermal state with an accuracy of 93.33% through images reporting the temporal profile of St, while the second algorithm

is a SVM classifier that succeeds in interpreting thermal sensation starting from physiological parameters with an accuracy of 90.6%.

In reference [38], the authors based their thermal comfort assessment on the computation of HRV due to its high correlation with the thermal environment. Supervised ML algorithms such as Logistic Regression (LR), Linear Discriminant Analysis (LDA), K-Nearest Neighbors (KNN), DT, Naïve Bayes (NB), SVM, RF have been trained to predict thermal comfort status of occupants, but among them SVM classifier reached the highest accuracy (93.7%) [38].

Although all the advantages that sensors and ML algorithms introduce in the thermal comfort assessment scenario, some limitations can be highlighted: first of all, it is possible to talk about manual data collection procedure due to the kind of sensors that have been used and for this reason the frequency with which data are recorded may be low. This leads to another issue which is the huge amount of time that may be spent and the fact that the measurement is not continuous and real-time. Moreover, the usage of wireless sensors (such as wearable ones) improves the experiment performance, but it can be a problem in terms of power supply [11], [14].

Hence, recent studies have designed thermal comfort assessment methods based on robotic systems in order to automatize the process and make the assessment continuously real-time.

#### **2.3.4 Robot-based measurement for thermal comfort assessment**

The technological progress that has characterized the last decades brought to the exploration of new methodologies for the improvement of thermal comfort assessment. Specifically, the real-time assessment of thermal sensation is the main target of the most recent scientific works together with a proper automatization of the process. For these reasons, it has been previously mentioned the importance that ML and AI are gaining in this scientific scenario due to their capability of predicting, analyzing and learning continuously new quantities [10]. However, the most innovative procedures are still local/manual based leading to poor efficiency during data collection and possible errors during data analysis [11]. Consequently, robot-based approaches have been introduced in this engineering field in order to obtain a continuous measurement of thermal comfort that is fully automatic and accurate. Thus, mobile robot platforms have been mostly

exploited to acquire data in a building using specific data acquisition systems, some degree of intelligence (machine learning algorithms) and interfacing them directly with the occupant. Environmental parameters such as  $T_a$ , RH, noise, air speed, are taken into account for the quantification of the building thermal conditions which in some studies are compared with the surveys that occupants should perform through the interaction with the robotic platform.

In the study conducted by Quintana B. [11], thermal comfort is evaluated with ComfBot. It is a movable robot platform that has been designed considering a hardware part with sensors, cameras (HD and RGB), odometry sensor and microphone array and a software part which exploits the open-source framework Robot-Operating System (ROS).

In [11], Wukong robot has been designed as AI environmental controller in order to study and predict thermal comfort through KNN algorithm. This last one predicts thermal comfort with an accuracy of 88.31% by using a large dataset that includes traditional PMV model outputs and the parameters detected with the robot sensors [10]. Furthermore, also in this study the interaction with the user is fundamental to trigger all the subsequent process. Indeed, Wukong shows a hardware and software part called voice interaction module, which enable the robotic system to ask occupants about their thermal feeling enriching the data set used for the thermal comfort prediction.

Ming Jin et al. [39] proposed in their research a novel “automated mobile sensing” system for indoor environmental quality monitoring. They developed a mobile robot in order to create an “active inference” procedure, where the robot plans its path in the building, detect environmental samples at locations of interests and monitor the indoor environmental quality in terms of air-change effectiveness (ACE), i.e. air distribution system’s ability to deliver ventilation air to a certain space. A spatio-temporal interpolation algorithm is employed in order to capture spatial and temporal dynamics and reconstruct continuous mapping of the indoor environment [39]. Several algorithms such as KNN, support vector regression (SVR), adaptive boosting (AdaBoost), RF and Extra Trees have been implemented in order to detect ACE local variation with high spatial granularity and accuracy [39].

## ***2.4 Limitations of the state of art***

From the analysis of the state of art, it emerges that thermal comfort assessment has been a real challenge in different scientific field due to its huge impact on building organization and maintenance and people's health. Indeed, it is clear how occupants' thermal sensation triggers physiological phenomena that in case of prolonged thermal discomfort impact negatively on humans' health and wellbeing. For these reasons, scientific research aimed to establish objective methodologies for thermal comfort assessment starting from both environmental and physiological parameters. However, despite the improvements of the proposed techniques, there are some limitations that make thermal comfort assessment still an open challenge.

Even though adaptive methods gave more relevance to human beings and to the physiological parameters for thermal comfort estimation, the tools and devices used for it are still too invasive. For instance, using ECG sensors for the heart rate acquisition can lead to annoying situations during the measurement procedure and it can also provoke uncertainty in the results since the quality of the performance depends on the operator skill and on how these sensors are placed. For this reason, the current work follows the recent trend of employing wearable sensors and infrared technologies to minimize the invasiveness and maximize the efficiency of the measurement.

This issue leads also to another observation that is mainly related to economic aspects. Indeed, a consistent part of thermal comfort studies have based their experimental setups on expensive devices such as thermal cameras or medical tools (ECG sensors, EEG sensors). Nevertheless, given the increasing importance of thermal comfort assessment in everyday life situation, affordable instrumentation should be integrated in this process. Hence, this work will demonstrate that low costs infrared sensors and wearable devices can substitute the traditional and more expensive instrumentations reaching the same consistent results in terms of thermal comfort quantification.

Another innovation that thermal comfort studies should introduce into people's everyday routine is a more user-friendly approach. Hence, robot-based methods have been developed in this engineering field. However, most of the studies reported in literature have considered and exploited robotic systems that analyzed exclusively objective environmental parameters without involving the subject. In other words, despite this

assessment procedures have improved the thermal monitoring of a building thanks to the precision and accuracy of the measurements, these methodologies are not user-centered. Hence, thermoregulation, physiological parameters and all the complications that thermal discomfort can provoke on people's health are not used, reducing these robot-based measurements to processes focused on the building efficiency and not on the occupant's wellbeing. For this reason, one of the main goals of this master thesis is the designing of a methodology which uses a robotic companion such as Misty II that can:

- detect and process physiological parameters and environmental factors;
- interface directly with the subject;
- give a real-time response based on the occupants' thermal sensation.

In conclusion, the current work tries to overcome all the issues characterizing the state of art at present, with the employment of a social robot which can understand whether a user is in thermal comfort or discomfort starting from the detection of environmental and physiological signals.

Moreover, the employment of low costs infrared sensors and wearable technologies is a remarkable characteristic of the whole project according to the need of reducing the invasiveness and the costs of tools by preserving and improving the efficiency of the performance. In this way, the designed method assigns the user a new level of importance since:

- he/she directly interfaces the problem;
- the problem can be managed by the user;
- the whole system is focused on the preservation and improvement of human health.

## CHAPTER 3: MATERIALS AND METHODS

This section is dedicated to a detailed description of the procedures implemented to achieve human thermal comfort assessment through a robot-based method.

The developed methodology is based on the acquisition of environmental and physiological parameters in a thermally-controlled indoor space through a specific measurement set-up of sensors that includes wearable devices, infrared (IR) sensors, and instrumentation to detect environmental parameters. Together with these tools, the social robot Misty is introduced to make the assessment more user-friendly and to achieve an automatic estimation. Finally, machine learning (ML) algorithms has been chosen, according to literature, as the most suitable approach for the computation and prediction of occupants' thermal sensation vote (TSV). Hence, in this section, it is possible to find the explanation of the phases that have been implemented during the practical part of this project with the aim of providing a proper amount of information to reproduce or improve the study.

In Fig. 5, it is possible to appreciate a general overview of the concept at the base of the implementation. In particular, the activities developed in the present work can be summed up through the following steps:

- *Measurement set-up*: all the above-mentioned sensors will convey the collected data to the single-board computer Raspberry Pi 4 Model B to obtain a single collection platform that communicate with the social robot Misty II. Hence, hardware connections and software communication are the principal targets of this phase.
- *Tests*: an experimental setup will be developed to assess the parameters for a proper thermal comfort estimation. The sensors that have been integrated into Misty II in the first phase will be used during a set of experiments, involving human participants.
- *Data analysis*: once all signals have been recorded during the tests phase, they are processed to obtain consistent results and to verify whether the collected parameters and the applied algorithm could provide an accurate estimation of the TSV. The data analysis step is divided into two different phases:

- The first one describes the software data flow logic at the base of the data acquisition protocol used during the tests.
- The second phase is the processing of the collected data that leads to the construction of the dataset used to train seven different ML algorithms chosen according to the literature. The aim of ML is to predict TSV with different accuracies.

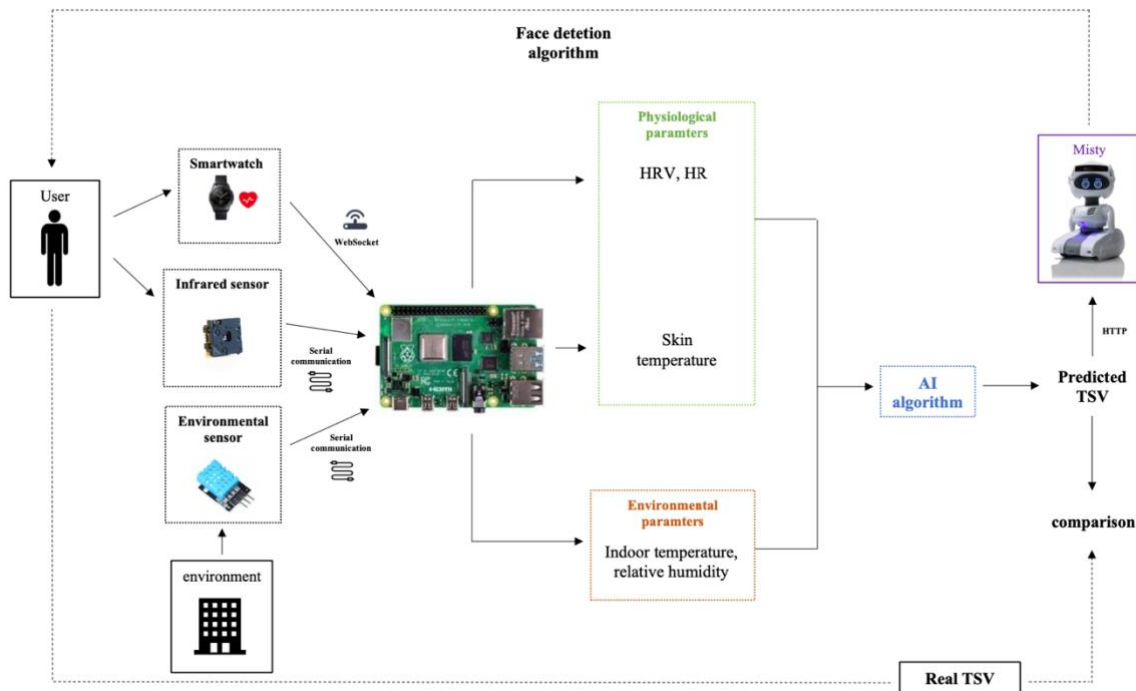


**Figure 5.** Block scheme describing the workflow of the overall research.

Before going deeper with the experimental setup and with the description of the computational process that leads to the TSV prediction, it is convenient to dedicate the following paragraph to a technical overview of all the sensors and electronic devices included in this project.

### ***3.1 SENSORS AND DEVICES***

In the current study, several sensors and hardware components have been involved to create a structure that can record environmental and physiological parameters. In particular, they are:

1. A Misty II social robot;
2. a portable Raspberry Pi 4;
3. a wearable device (Samsung Galaxy Watch);

4. a sensor for the measurement of air temperature and relative humidity (DHT11);
5. an IR sensor (Flir Lepton 3.5).

A more detailed description of each component is provided in the following sections.

### **3.1.1 Sensorized Robot (Misty II)**

At present, the most recent approach to thermal comfort assessment involves robotic systems due to the possibility to enrich their skills and capabilities with the integration of additional tools such as sensors and microcontrollers. Moreover, the introduction of robots in the thermal comfort scenario facilitates the interaction with the user which becomes fundamental for the measurement.

Consequently, it has been chosen to exploit robotic functionalities for a more accurate and personalized assessment. Misty II by Misty Robotics has been selected given its capability to interact with people through its speaking skills and gestures. Moreover, based on the heterogeneous set of sensors that characterizes its structure, the robot can localize itself inside a building (SLAM), it can recognize a human face through the face detection skill, and can move with confidence thanks to the bump sensors. It is also possible to extend its hardware structure with any needed sensor through the integration of devices such as Arduino or Raspberry Pi and specific programming language can be used when new robotic skills are needed.

The set of sensors installed on Misty II includes 6 capacitive touch sensors, 8 time-of-flight sensors, and 10 bumps sensors. The first ones are proximity sensors, and they are placed on Misty's head and chin. They allow Misty to perceive a nearby object or something that is touching it. These sensors use six pieces of thin foil under the plastic shell connected to a sensor controller. When a conductive object (such as a finger) comes close to the foil, there is a capacitive coupling between the foil and the detected object.

The time-of-flight sensors allow Misty to measure the distance between its position and the nearest obstacle. Misty uses eight time-of-flight sensors (three front, one rear, and four facing downward) to calculate the distance of objects in her path and let it understand if it is about to fall when it reaches an edge. In other words, they allow Misty to move in an environment with confidence. For instance, when the robot is near an edge and risks falling, Misty movements are stopped at 0.15 meters from the danger. Moreover, the time-of-flight sensors are linked to the 10 bump sensors placed at the base of the robot. They

are used in case of collision between the robot and an object. Finally, there are the occipital structure core depth sensors placed in the head of the robot which includes:

- 166° diagonal field of view wide-angle;
- dual IR cameras;
- an Inertial Measurement Unit (IMU);
- 4K RGB camera.

This set of sensors is used for 3-D map creation and for the facial recognition skill that has been mentioned before. A more detailed overview of all the sensors included in Misty II hardware structure can be appreciated in Fig. 6.



**Figure 6.** Misty II on-board sensors.

### 3.1.2 Single-Board Computer

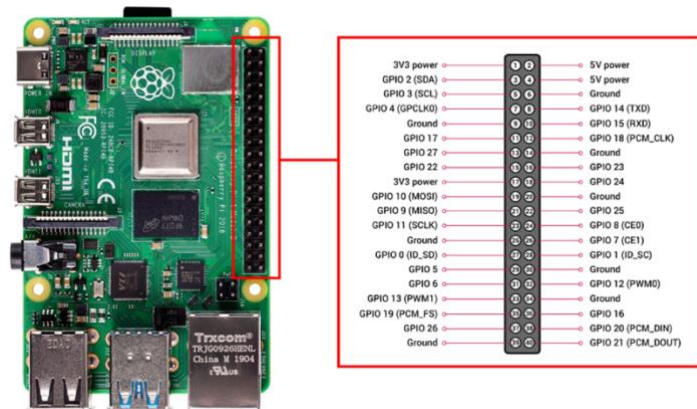


**Figure 7.** Raspberry Pi 4 model B and its GPIO pins.

Raspberry Pi is a single-board computer (SBC) that is mostly used to develop programming skills or to build hardware projects thanks to its easy-to-use interface. It is possible to find different versions and models of the board. Indeed, the Raspberry Pi model can go from 1 to 4 and its versions can be A, B, or the more advanced version B+. Raspberry presents different peripherals: mouse, keyboard, Wi-Fi adapters can be connected using its four USB 2.0 ports and all kinds of monitors can be connected thanks to the HDMI ports. If all these peripherals are used, Raspberry becomes a full-size computer. Furthermore, the board presents an Ethernet port for network connection and 40 general-purpose input/output (GPIO) pins to control electronic components such as physical sensors and other devices (LEDs, modules, boards) (Fig. 7). Since Raspberry is the basic component of a computer, naïvet is possible to install several operating systems such as Raspbian thanks to an SD card present on the board. It is possible to observe a more detailed and intuitive description of the Raspberry Pi hardware components in Figure 7. These numerous features enable the users to exploit Raspberry in a wide range of use cases. For instance, in literature, it is possible to find lots of research concerning healthcare applications where this single-board computer is employed to design new instruments from scratch or to add new functionalities to an already existing device [40]. In section 2, it has been mentioned a study where a robotic system has been created to assess thermal comfort through the detection of environmental factors characterizing the analyzed indoor space. In order to do that a Raspberry Pi 4 has been used as the core of the built robotic architecture [10]. Based on the functionalities and the efficiency

characterizing this single board computer, Raspberry Pi 4 Model B has been chosen in this project as the board for a correct and reliable sensor integration procedure.

### 3.1.3 Smartwatch

According to literature, thermal comfort assessment has introduced wearable sensors to reduce the invasiveness of the measurement procedure when physiological parameters have to be acquired. The present work follows this innovative trend to make the assessment more comfortable for the subject and to record data in a more accurate way. For these reasons, the smartwatch Samsung Galaxy Watch has been employed in the current thesis (Fig. 8). Firstly, a benchmark analysis has been conducted with the aim of finding a smartwatch or a smart band which:

- was able to assess physiological parameters such as heart rate, ppg signal, skin temperature;
- allowed the operator to extract and handle those data;  
was characterized by an open-source operating system.

Among all the found options, the Samsung Galaxy Watch was selected to collect occupants' biometric data. Indeed, it respects the three main features that have been just mentioned. This smartwatch is a mid-range wearable device with Tizen 4.0 operating system which includes an advanced heart monitoring system that can help to improve everyday habits. The smartwatch is equipped with a PPG sensor capable of extracting the heartbeat based on the changes in the skin's light absorption. The choice of using the Samsung Galaxy Watch is supported also by literature. In fact, it emerged that some scientific studies have already used it in the case of thermal comfort assessment reaching reliable and accurate results [41].



**Figure 8.** Samsung Galaxy Watch.

**Table 1.** Technical information of the smartwatch employed in this study (Samsung Galaxy Watch).

| <i>Technical information</i>               |  |
|--|--|
| <i>On-board sensors</i>                    | Accelerometer, gyroscope, barometer, ambient light sensor, optical sensor (PPG sensor) |
| <i>Monitoring targets</i>                  | Heart rate, blood pressure, sleep quality, physical activity                           |
| <i>Sampling frequency for PPG data</i>     | 100 Hz   |
| <i>Sampling frequency for RR intervals</i> | 10 Hz  |
| <i>Connectivity</i>                        | 3G/LTE, Bluetooth 4.2, Wi-Fi, Near Field Communication (NFC), GPS                      |
| <i>Operative System</i>                    | Tizen based Wearable OS 4.0  |

### 3.1.4 Environmental sensor

It is known that the basic parameters for a proper thermal comfort assessment are related to the environment. Specifically, indoor air temperature ( $t_a$ ) and relative humidity (RH) are the most important ones. In the current work, the low-cost environmental sensor DHT11 has been chosen for this purpose. DHT11 is a basic, digital sensor that uses a capacitive humidity sensor and a thermistor connected with an 8-bit microcontroller to measure the surrounding air. It gives as output a digital signal (Fig. 9). The sensor is also factory calibrated and hence easy to interface with other microcontrollers. It can measure temperatures from 0 °C to 60 °C and humidity from 20% to 90% with an accuracy of  $\pm 2$  °C and  $\pm 2$  %, respectively (Tab. 1). Only three pins are available for use: VCC (Voltage Common Collector), GND (Ground), and DATA (Fig. 9). The communication process is triggered with the DATA line sending start signals to DHT11. Once DHT11 receives the signals, it returns an answer signal. The hardware components and the mentioned technical specifications ensure high reliability and excellent long-term stability of the sensor. Thus, it has been chosen for this study accordingly also to the low cost that it has.

**Table 2.** Technical specifications of DHT11.

| <i>Specification</i>                    | <i>Range</i> |
|---|--------------|
| <i>Humidity measurement</i>             | 20 – 90% RH  |
| <i>Temperature measurement</i>          | 0 – 60 °C    |
| <i>Working voltage</i>                  | 5V           |
| <i>PCB size</i>                         | 2.0 x 2.0 cm |
| <i>Humidity measurement accuracy</i>    | ±5% RH       |
| <i>Temperature measurement accuracy</i> | ±2 °C        |

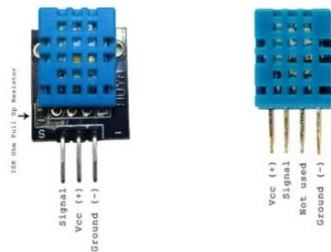


**Figure 9.** DHT11 and its pins. It is possible to appreciate that there are two kinds of DHT11 depending on the number of pinouts.

### 3.1.5 Infrared sensor

The level of invasiveness reached during thermal comfort measurement is one of the main issues that the scientific community is trying to overcome with the introduction of new devices and sensors. This problem occurs when physiological parameters such as heart rate (HR) or skin temperature need to be assessed to get a personalized thermal comfort estimation. For this reason, nowadays wearable sensors, infrared (IR) sensors, and thermal cameras are widely used. Furthermore, scientific literature affirms that among the physiological parameters involved in the thermal comfort measurement, skin temperature is one of the most reliable features to use to achieve an acceptable thermal comfort estimation. Consequently, IR imaging is exploited in the current work to assess this parameter. After a benchmark analysis and deep literature research, it emerged that Flir Lepton 3.5 infrared sensor would be the most suitable tool for skin temperature detection due to its low cost and high resolution. Moreover, this sensor has been used together with its easy-to-interface evaluation board (Breakout Board v2.0) to quickly connect the Flir Lepton camera module to a common platform such as Raspberry (Fig. 10).

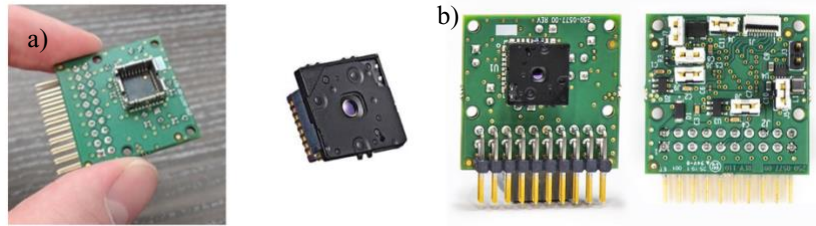


**Figure 10. (a) Lepton 3.5 and its Breakout Board v2.0. (b) The IR sensor inserted in its board.**

**Table 3.** Technical specifications of Flir Lepton 3.5.

| <i>Technical specifications</i>   |  |
|-----------------------------------|--|
| <i>Sensor Technology</i>          | Uncooled Vox microbolometer  |
| <i>Spectral Range</i>             | Longwave infrared, 8 $\mu\text{m}$ to 4 $\mu\text{m}$  |
| <i>Array Format</i>               | 160x120, progressive scan  |
| <i>Pixel size</i>                 | 12 $\mu\text{m}$   |
| <i>Effective Frame Rate</i>       | 8.7 Hz   |
| <i>Thermal Sensitivity</i>        | < 50 mK (0.050 $^{\circ}\text{C}$ )  |
| <i>Temperature compensation</i>   | Automatic. Output image independent of camera temperature.   |
| <i>Radiometric Accuracy</i>       | High gain Mode: Greater of +/- 5 $^{\circ}$ C or 5% (typical) Low Gain Mode: Greater of +/- 10 $^{\circ}$ C or 10% (typical)   |
| <i>Non-uniformity corrections</i> | Integral Shutter   |
| <i>Scene Dynamic Range</i>        | High Gain Mode: -10 $^{\circ}$ to +140 $^{\circ}$ C<br>Low Gain Mode: -10 $^{\circ}$ to +400 $^{\circ}$ C (at room temperature), -10 $^{\circ}$ to +450 $^{\circ}$ C (typical) |
| <i>Image optimization</i>         | Factory configured and fully automated   |
| <i>FOV -horizontal</i>            | 57 $^{\circ}$  |
| <i>FOV -diagonal</i>              | 71 $^{\circ}$  |
| <i>Lens Type</i>                  | f/1.1  |
| <i>Output Format</i>              | User-selectable 14-bit, 8-bit (AGC applied), or 24-bit RGB (AGC and colorization applied)  |
| <i>Solar Specifications</i>       | Integral   |

Lepton 3.5 has a 160x120 resolution, uncooled Focal Plane Array (FPA), and offers calibrated radiometric output for the entire 19.200 pixels array. Lepton 3.5 has a thermal range of 400 °C providing even greater flexibility for demanding applications. Moreover, the new radiometric Lepton 3.5 provides advanced capabilities where temperature values and high-temperature scenes are required. In Tab. 2, all the principal technical specifications can be observed.

### 3.2 MEASUREMENT SETUP

In this paragraph, a technical description of the measurement setup will follow. In particular, it will be described the procedure of integration performed with the sensors reported in Tab. 3. They will be connected with the single board computer Raspberry which in turn will communicate with the social robot Misty II.

**Table 4.** Devices integrated with Raspberry Pi 4 and Misty II.

| <i>Device</i>               | <i>Measured parameter</i>                                   | <i>Technical information</i>   |
|-----------------------------|---|--|
| <i>Smartwatch</i>           | HRV   | Accuracy: $\pm 4$ ms at rest   |
| <i>Infrared Sensor</i>      | Skin temperature  | Resolution: 160x120<br>Thermal sensitivity < 50 mK                                   |
| <i>Environmental sensor</i> | Air temperature ( $t_a$ ) and<br>Relative Humidity ( $RH$ ) | Temperature accuracy: $\pm 2^\circ\text{C}$<br>Relative Humidity accuracy: $\pm 2\%$ |

It is possible to state that the central role of the integration process is performed by the Raspberry Pi 4 since it is the key element for an efficient hardware connection between all the sensors and for the interaction with the robot through specific communication protocols. Furthermore, the whole system is managed through Python codes which allow the Raspberry to receive and extract data from the sensors and also to implement the ML algorithm exploited in this study to predict the subject's TSV.

### 3.2.1 Measurement setup procedure

DHT11 and Lepton 3.5 have been connected to the Raspberry through serial communication. In particular, the GPIO pins of the Raspberry have been exploited (Fig. 3). The technical documentation of both the IR sensor and the environmental sensor has been consulted. Indeed, their datasheets supply a precise description of the GPIO pins disposition on the devices, and accordingly they also explain the configuration that the jumper wires should have to properly connect the sensors. By following this instruction, in the current work, the DHT11 has been connected through three female-to-female jumper wires as reported Tab. 4 and Fig. 11.

**Table 5.** DHT11 pins and the correspondent Raspberry GPIO pins.

| <i>DHT11</i> | <i>Raspberry Pi GPIO pin</i> |
|--------------|------------------------------|
| VCC          | 3.3V                         |
| DATA         | GPIO4                        |
| GND          | GND                          |

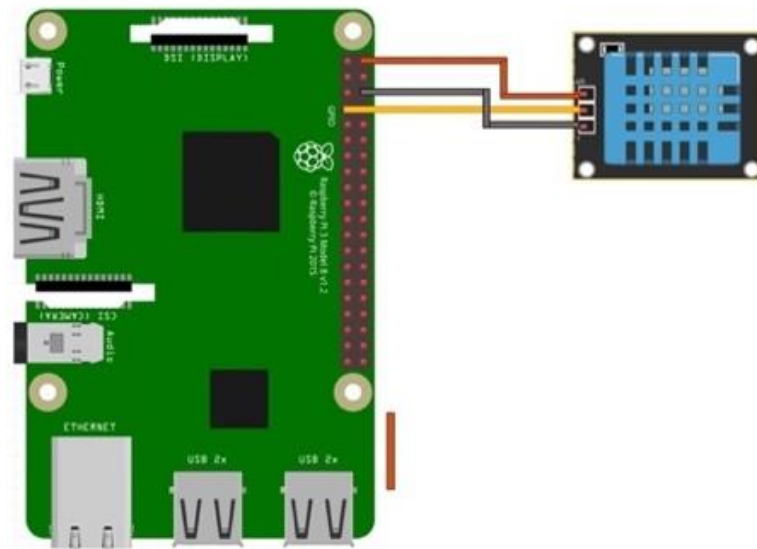


**Figure 11.** Visual representation of DHT11 connection with Raspberry Pi 4.

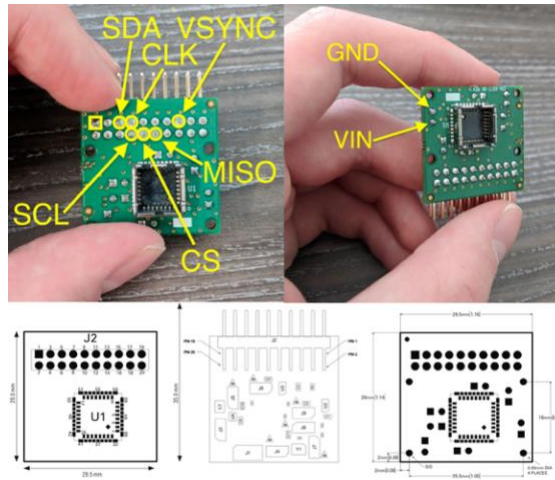


**Figure 12.** Pins configuration of the Breakout Board v2.0.

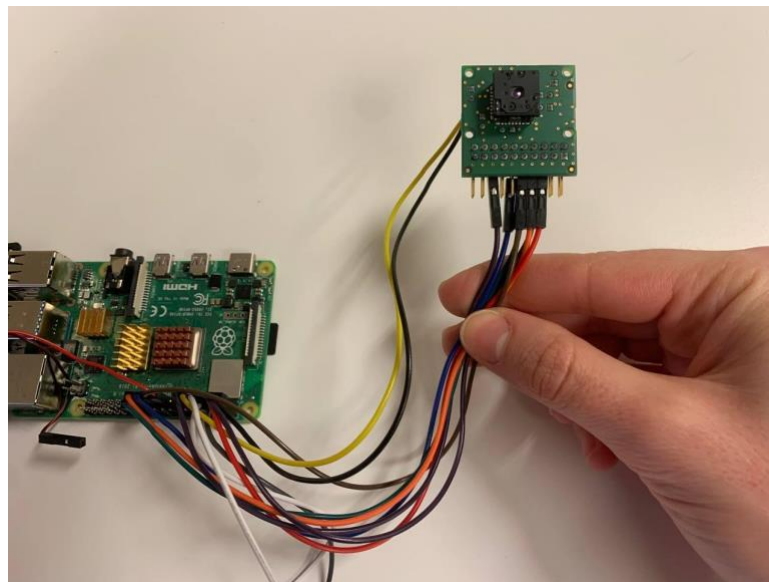


**Figure 13.** The Lepton module setup developed in the current work.

The Lepton 3.5 instead has been firstly inserted in its Breakout Board v2.0. As shown in its datasheet, this board has specific extremities (Fig. 12) where nine female-to-female jumper wires have been attached providing the proper connection with the Raspberry Pi 4 (Fig. 13). In the following table (Tab. 5), it is possible to appreciate which Breakout Board pins have been considered and to which Raspberry GPIO pins have been connected.

The present work acquires physiological data such as HR and HRV with the smartwatch Samsung Galaxy Watch (Tab. 3). To receive these relevant parameters, the smartwatch and the Raspberry Pi integration have been managed through the WebSocket communication protocol.

**Table 6.** Pins configuration for Lepton 3.5 and Raspberry Pi 4 connection.

| <i>Breakout board v2.0 pin</i> | <i>Function of Breakout board v2.0 pin</i> | <i>Raspberry Pi GPIO pin</i> |
|--------------------------------|--|------------------------------|
| J2 Pin 8                       | SCL  | GPIO 3                       |
| J2 Pin 7                       | SPI_CLK                                    | GPIO 11                      |
| J2 Pin 9                       | SPI_MOSI                                   | GPIO 10                      |
| J2 Pin 5                       | SDA  | GPIO 2                       |
| J2 Pin 10                      | CS   | GPIO 8                       |
| J2 Pin 12                      | SPI_MISO                                   | GPIO 9                       |
| J2 Pin 15                      | VSYNC                                      | GPIO 7                       |
| P1                             | GND  | GND                          |
| P2                             | VIN  | 3.3V                         |

Specifically, a dedicated application was developed and installed on the wearable device (Fig. 14). This app has been developed with the JavaScript-based software Tizen Studio. Its aim is detecting and collecting HR and HRV by exploiting the PPG sensor placed in the back of the smartwatch. Then, these data are sent to any device provided of an Internet Protocol (IP) address through the previously mentioned protocol (Fig. 15). In this specific case, HRV and HR are sent to the Raspberry Pi 4 once both the smartwatch and the single board computer have been connected to the same network.

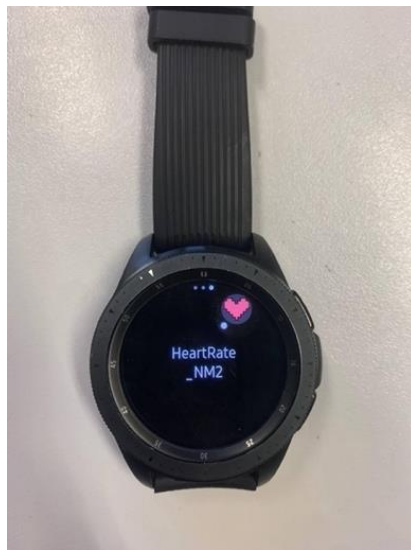


**Figure 14.** The application “HeartRate\_NM2” developed in the current work.

```

// WEBSOCKET
var websocketUrl = 'ws://172.20.10.8:8085';
var websocket = new WebSocket(websocketUrl);

websocket.onopen = function(e) {
  console.log('FUNZIONA TUTTO, readyState: ' + e.target.readyState);
};

websocket.onerror = function(e) {
  console.log('NON FUNZIONA NIENTE, readyState: ' + e.target.readyState);
};

websocket.onclose = function(e) {
  console.log('SÈ CHIUSO, readyState: ' + e.target.readyState);
};

console.log(websocket.readyState);

function sendMessage(msg) {
  if (websocket.readyState === 1) {
    websocket.send(msg);
  }
}

```

IP address

Data are sent to the device

**Figure 15.** Extract of the JavaScript code of the smartwatch application.

### 3.2.2 Software integration

Once all the mentioned devices have been integrated with the Raspberry Pi 4, it is needed an explanation of the Python codes implemented to manage this hardware structure and to control all the mentioned communication processes. Indeed, in this section, it will be possible to understand how HR, HRV, skin temperature,  $t_a$  and RH are acquired and processed on the Raspberry Pi 4 and how they are used for the TSV estimation.

#### 3.2.2.1 Environmental sensor

In order to use DHT11 with the Raspberry, the *adafruit\_DHT* library has been installed and used in the Integrated Development Environment (IDE) used for Python coding on Raspberry. Indeed, this library encloses all the functions that allow the acquisition and visualization of  $t_a$  and RH. Hence, this library has been exploited in the current work to create a function that gives as output the above-mentioned environmental parameters. In Fig. 16 it is possible to appreciate an extract of the python code used for this purpose.

```

import time
from board import D4
import adafruit_dht

def get_env_params():
    dhtDevice = adafruit_dht.DHT11(D4)

    temperature=dhtDevice.temperature
    humidity=dhtDevice.humidity

    return temperature, humidity

```

**Figure 16.** Extract of the Python code for “Get\_env\_params” function implementation.

### 3.2.2.2 Infrared sensor

The current project has included the IR sensor Lepton 3.5 to measure subjects' skin temperature. In order to accomplish this task, the *v4l2lepton3* Python package realized by [42] has been installed and exploited. Specifically, it is a pack of tools that allows to control the camera over the Integer Integrated Circuit (I2C) interface, capture and save individual frames and stream live thermal videos over Transmission Control Protocol (TCP). Thus, the *v4l2lepton3* library has been chosen for the current work to acquire subjects' skin temperature and control the IR sensor. In particular, the function reported in Fig. 17 has been developed. In particular, it:

- Takes a thermal image through the integrated Lepton sensor;
- Computes the mean skin temperature from a specific Region of Interest (ROI) that in the current study is the subject's forehead.

Before the thermal image acquisition, the Raspberry has been configured according to the sensor needs. Hence, both the I2C and the Serial Peripheral Interface (SPI) have been enabled together with the Raspberry Camera interface.

```
def get_temp():
    capturer = Lepton3Capturer('/dev/spidev0.0')
    #faces=detect_faces(ip_misty)

    with capturer:

        frame=capturer.get_frame(timeout=5)
        plt.imshow(frame)
        #frameinlista=frame.tolist()

        #roi=frame[25:100,40:95] -> forehead
        roi=frame[18:25, 60:70]
        plt.imshow(roi)
        roiCels=(roi/100)-273.15
        temp_mean=np.mean(roiCels)

    return temp_mean, frame
```

**Figure 17.** Extract of the “get\_temp” Python function implemented for the current work.

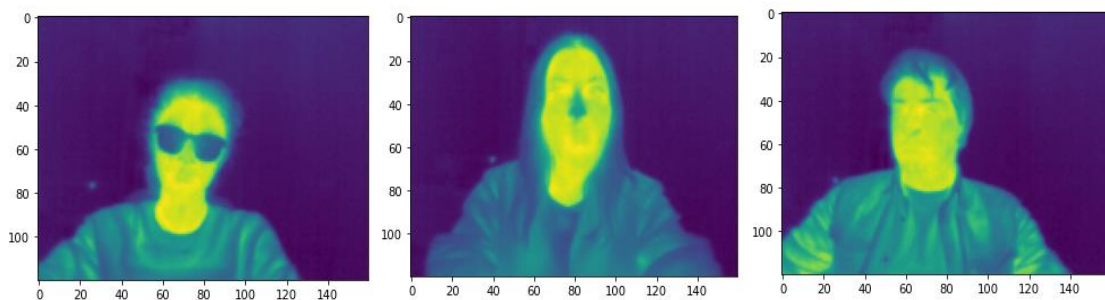


**Figure 18.** Three examples of IR frames captured by Lepton 3.5.

### 3.2.2.3 Smartwatch

In the previous paragraphs, it has been explained that smartwatch and Raspberry have been integrated using an application that exploits WebSocket protocol to send HR and HRV data to an external device. However, it is worthy attention to the Python code that has been developed in the Raspbian environment to receive those data. Specifically, the Python code includes several functions that aim at:

- opening a connection between the server (Raspberry) and the client (smartwatch);
- creating an SQLite database where the data received through WebSocket protocol can be stored;
- closing the connection with this database.

In Fig. 19 it is possible to appreciate an extract of the Python codes implemented for this purpose.

```
def db_connect(db_name):
    global conn
    global c

    conn = sqlite3.connect(db_name)
    c = conn.cursor()
    c.execute("""CREATE TABLE IF NOT EXISTS session
              (session_id INTEGER PRIMARY KEY AUTOINCREMENT, name TEXT,
              ts TIMESTAMP DEFAULT CURRENT_TIMESTAMP)""")
    c.execute("""CREATE TABLE IF NOT EXISTS measurement
              (measurement_id INTEGER PRIMARY KEY AUTOINCREMENT,
              session_id INTEGER, hr real, hrv real, q real,
              air_temp real, air_rh real, co2 real,
              ts TIMESTAMP DEFAULT CURRENT_TIMESTAMP)""")

    return conn

def db_newsession(name):
    global conn
    global c

    print(name)
    c.execute("INSERT INTO session(name) VALUES (?)", (name, ))
    last_row_id = c.lastrowid
    conn.commit()
    return last_row_id

def db_savedata(session, val):
    global c

    c.execute("INSERT INTO measurement(session_id, hr, hrv, q) VALUES (?, ?, ?, ?)", (session, val["hr"], val["hrv"], STATE["value"]))

def db_commit():
    global c

    conn.commit() # save changes

def db_close():
    global conn
```

**Figure 19.** Extract of Python code where several functions have been implemented in order to exploits Samsung Galaxy Watch collected data.

## 3.3 TESTS

Once all the devices have been integrated and the communication within them and Misty has been established, it is necessary to test the whole system through a specific experimental procedure. In order to do that, a room of the the DIISM (Dipartimento di Ingegneria Industriale e Scienze Matematiche) of the Università Politecnica delle Marche

has been chosen. Its dimensions are 4.8 m (length) × 2.9 m (width) × 3.0 m (height) and its planimetry is visible in Fig. 20.

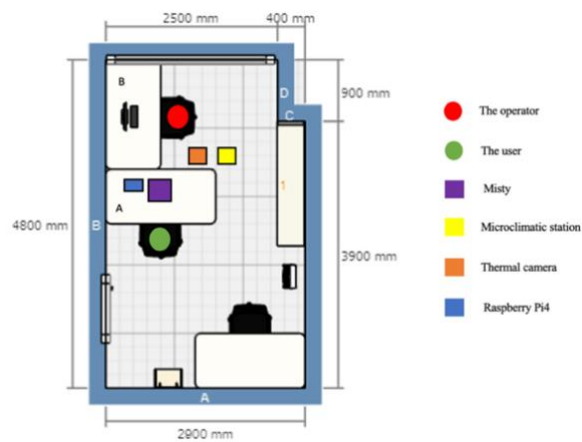


**Figure 20.** Planimetry of the room used for the experimental procedure. It is also possible to appreciate how some devices have been placed inside the room.

In this indoor space, all the devices and instruments needed for the thermal comfort assessment have been placed. Misty II has been placed on desk A (Fig. 20, Fig. 21) at 60 cm from the edge that interfaces the chair where the subject will be sitting. Misty is put on its base and the Raspberry is placed next to it. As regards the two sensors wired to the Raspberry, the environmental sensors DHT11 has a fixed position, while the breakout board with the inserted IR sensor (Lepton 3.5) is attached at the level of Misty’s chest (Fig. 21).

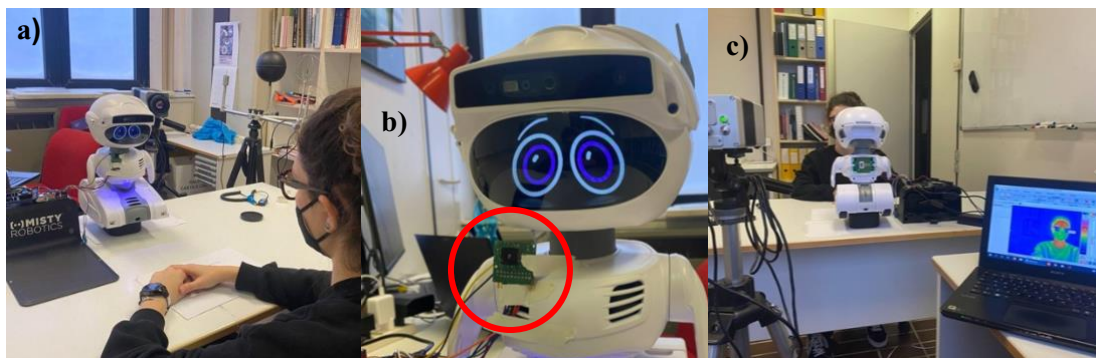


**Figure 21.** Pictures of how the indoor space has been organized during the trials. In the second image (b) it is possible to see how and where the Lepton module has been attached (red circle).

This position has been chosen so that the Lepton 3.5 is centred on the subject’s face. In fact, the subject will be sitting on a chair that is aligned with Misty’s position. In order to validate all the measurements performed by the low-cost sensors described in the previous

paragraphs, other standard instrumentations have been included in the experimental setup (Fig. 22).



**Figure 22.** (a) Microclimatic station; (b) 39ultiparametric belt; (c) temperature sensor iButton; (d) thermal camera.

They are:

- the microclimatic station DeltaOhm 32.1 (Fig. 22 a) to assess RH,  $t_a$  and air velocity  $v_a$ ;
- The multiparametric belt BioHarness 3.0 (BH3) to assess HRV of the subjects (Fig. 22 b);
- The thermal camera VarioCam HD to assess participants' face temperature (Fig. 22 c);
- two temperature sensors iButton D1922 to assess both indoor  $t_a$  and the subject's skin temperature (Fig. 22 d).

The experimental protocol has been applied during three different days and it has been organized as follow:

- *Cold discomfort trial*: 10 subjects enter the room where the temperature has been previously decreased at 14 °C to make them feel cold (Fig. 23). According to the norms ASHRAE 55 [2], UNI EN ISO 7730 [3], and ISO 17772 [43], this is the temperature at which a person can experience cold thermal discomfort.
- *Warm discomfort trial*: the same 10 subjects enter the room where the temperature has been increased up to 28 °C (Fig. 23) to make occupants feel uncomfortable

according to the norms. Thus, during this test subjects should experience hot thermal discomfort [2], [3], [43].

- *Comfort trial*: in this case the room has been thermally prepared to let the 10 subjects feel comfortable during the experiment. Hence, accordingly to [2], [3], [43], the temperature has been maintained at 21° (Fig. 23).

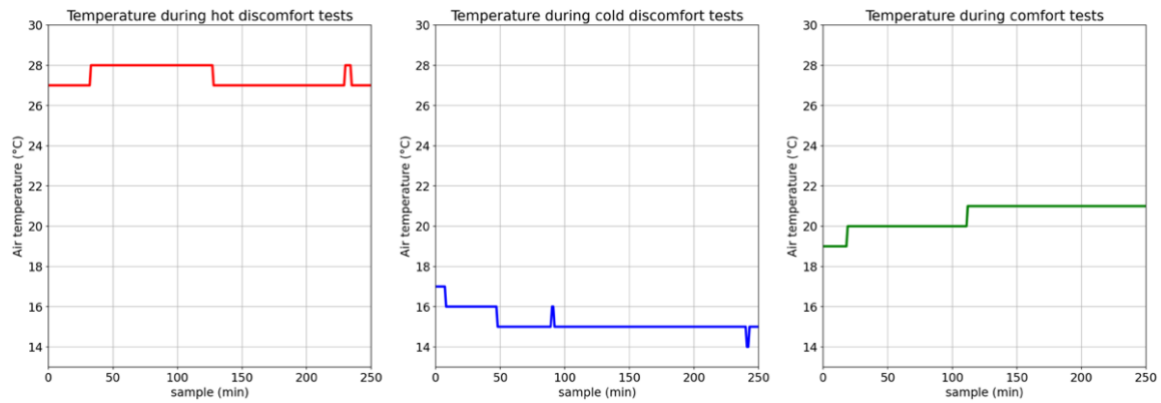


**Figure 23.** Trend of the environmental temperature reached during the three trials.

The measurement procedure developed during these three trials is the same and it has lasted 12 minutes. The only aspect that has been modified is the  $t_a$ . In particular, the experimental protocol has been developed through the following steps:

- Before entering the room, the subject is asked to wear the smartwatch Samsung Galaxy Watch on the non-dominant wrist, the BH3 on the chest, and one of the iButton sensors under the back of the smartwatch.
- The subject is asked to communicate the TSV before entering the room.
- The subject enters the room and communicates once again his/her TSV.
- The subject sits in front of Misty accordingly to the disposition given to the whole experimental setup (Fig. 20). Moreover, the subject has to maintain the position fixed for the entire procedure.
- The data acquisition protocol starts for five minutes.
- At the end of this period, the subject is asked to communicate his/her TSV.
- The data acquisition protocol is repeated for 5 minutes.
- The subject communicates his/her TSV.

All these activities are monitored by the operator that stays inside the testing room to verify and solve any malfunctioning during the tests. The role of the operator is also to

ask the participant to communicate his/her TSV accordingly to the above-described protocol.

### 3.3.1 Participants

The experimental procedure has involved the same 10 subjects for all three days of trials. The participants were 7 females and 3 male subjects, and their anthropometric features are reported in Tab. 6. All the participants were not subjected to a clothing regime: they were simply asked to wear their everyday clothing. In this way, more realistic results can be obtained since human beings have a different thermal sensation when wearing different clothes. Hence, this condition guarantees the subjectivity of the tests.

**Table 7.** Anthropometric features of the participants.

| <i>User</i> | <i>Gender</i> | <i>Age</i> | <i>Height (cm)</i> | <i>Weight (Kg)</i> | <i>BMI</i> | <i>Attended trial</i> |
|-------------|---------------|------------|--------------------|--------------------|------------|-----------------------|
| 1           | F             | 25         | 169                | 53                 | 18.56      | 1, 2 ,3               |
| 2           | M             | 22         | 184                | 74                 | 21.86      | 1, 2 ,3               |
| 3           | M             | 29         | 187                | 108                | 30.88      | 1, 2 ,3               |
| 4           | F             | 25         | 168                | 66                 | 23.38      | 1, 2 ,3               |
| 5           | F             | 28         | 165                | 65                 | 23.88      | 1, 2 ,3               |
| 6           | F             | 28         | 165                | 65                 | 23.88      | 1, 2 ,3               |
| 7           | M             | 27         | 178                | 72                 | 22.72      | 1, 2 ,3               |
| 8           | F             | 25         | 168                | 57                 | 20.19      | 1, 2 ,3               |
| 9           | F             | 24         | 168                | 56                 | 19.84      | 1, 2 ,3               |
| 10          | F             | 24         | 167                | 53                 | 19.00      | 1, 2 ,3               |

### 3.4 DATA ANALYSIS

In this section, the software procedure applied during the study will be described. In particular, the software logic at the base of the whole process can be organized into two

main parts. The first part includes the software dataflow that has driven the real-time data acquisition protocol during the trials, while the second part is focused on the processing of the collected data to perform a thermal sensation vote prediction in post-processing.

### 3.4.1 Measurement procedure and software dataflow

The current paragraph describes the logic that rules on the data acquisition protocol applied during the experimental procedure described in section 3.3. The final goal is an attempt of real-time TSV prediction once HR, HRV, skin temperature,  $t_a$ , and  $RH$  are acquired. In fact, when all these relevant variables have been measured, a ML algorithm will be exploited to process them and obtain a predicted TSV. The code has been developed once again in the Raspbian environment (Raspberry Pi operating system) and a general overview of the performed passages is reported in Fig. 24.

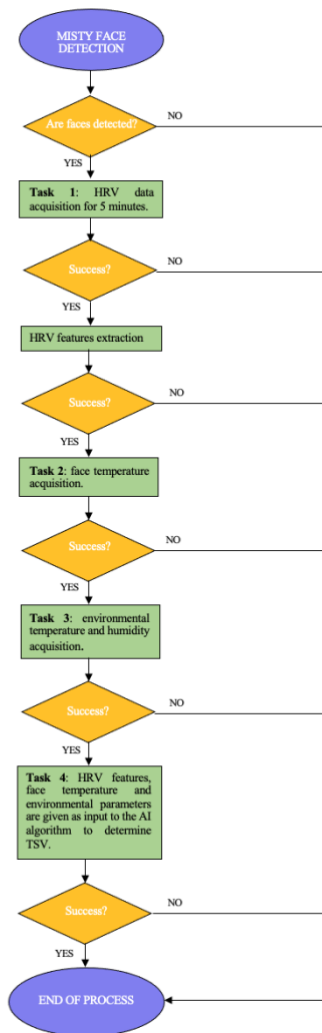


**Figure 24.** Flowchart of the logic at the base of the Python code for real-time TSV prediction.

As it is possible to appreciate, the first step is a face detection procedure performed by Misty II. In fact, it has been decided to use a face detection algorithm as the trigger event for the whole process: Misty II has to recognize the person in front of it, and then the procedure can start.

```

API_ENDPOINT = 'http://' + ip_misty + '/api/cameras/rgb?base64=true&fileName=nicole&width=320&height=240&displayOnSc
r = requests.get(url = API_ENDPOINT)
data = r.json()
my_img = data['result']
my_img = my_img['base64']
im = Image.open(BytesIO(base64.b64decode(my_img)))
image_np = np.array(im)
plt.imshow(image_np)

# cascPath = "haarcascade_frontalface_default.xml"
faceCascade = cv2.CascadeClassifier(cv2.data.haarcascades + 'haarcascade_frontalface_default.xml')
gray = cv2.cvtColor(image_np, cv2.COLOR_BGR2GRAY)

# Detect faces in the image
faces = faceCascade.detectMultiScale(
    gray,
    scaleFactor=1.1,
    minNeighbors=5,
    minSize=(30, 30),
    flags = cv2.CASCADE_SCALE_IMAGE
)

print("Found {} faces!".format(len(faces)))
found_faces = len(faces)
# Draw a rectangle around the faces
color = (255, 0, 0)
for (x, y, w, h) in faces:
    cv2.rectangle(gray, (x, y), (x+w, y+h), color, 4)
    top_left=(x,y)
    bottom_right=(x+w, y+h)

plt.imshow(gray)
cv2.imshow("Faces found", gray)

```

 HTTP Get request  
 Haar-Cascade Algorithm for face detection

**Figure 25.** Extract of “face\_detect” function used as first step of the whole workflow.

```

####FACE DETECTION
ip_misty = '172.20.10.6'
faces = detect_faces(ip_misty)

####if faces are detected
if faces > 0:
    ### 1) acquisition of hrv for 5 minutes
    print("Starting server on {}...".format(get_ip()))
    loop = asyncio.get_event_loop()
    db_connect('ciaone.sqlite')
    watch_server = loop.run_until_complete(websockets.serve(watch, '0.0.0.0', 8085))

    try:
        loop.run_forever()
    except KeyboardInterrupt:
        print("i'm here")

    print('feature computation')
    file=pd.read_csv('galaxy_data.csv', sep = ';')
    print(file)

    hrv = file['HRV']
    hr = file['HR']
    time=file['timestamp']
    time_in=time[0]
    time_fin=time[len(time)-1]
    my_hrv = hrv.to_list()

    print(my_hrv)
    print(type(my_hrv))

    print('start')

```

**Figure 26.** Python code extract of the first part of data acquisition phase.

Specifically, the function reported in Fig. 25 has been created. It has been based on the Hypertext Transfer Protocol (HTTP) communication. Indeed, a HTTP GET request is sent to the robot. This request asks Misty to take a picture of the subject that should be in front of it. In this picture, the Haar-Cascade face detection algorithm is employed as reported in the code extract (Fig. 25). The output of the function is the number of found faces. Thus, if this number is different from zero the process can go on with the next step (Fig. 26), which is the HRV and HR acquisition from the smartwatch. In order to detect the subject's HRV, this python code exploits the functions mentioned in the previous section. Indeed, a connection between the server (Raspberry) and the client (the smartwatch) is created and data are acquired and stored in an SQLite database (Fig. 26). The HRV acquisition lasts five minutes, at the end of which the collected data are used for HRV features extraction. For this operation, an additional function called "get\_hrv\_features" has been implemented. Through its usage, the mean value of HRV and the median of the HRV have been calculated.

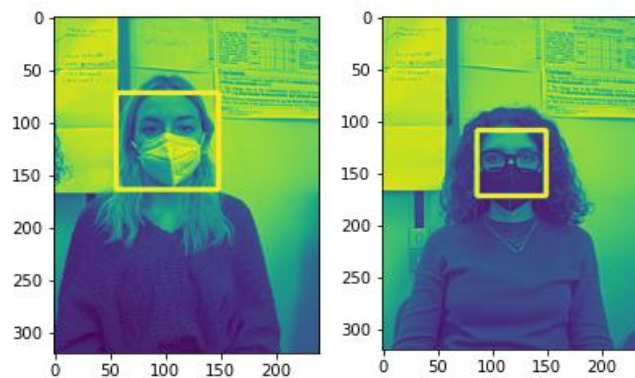


**Figure 27.** Two examples of face detection output performed by Misty II. The rectangle identifies the subjects in front of the robot.

If this phase has been successful, face temperature acquisition can start. In particular, the IR sensor Lepton 3.5 is exploited. The python function in Fig. 17 is used and it gives as output the captured frame and the mean temperature computed on a fixed Region of Interest (ROI) centered on the subject's forehead. After that, the third task can start (Fig. 24). As reported in the flowchart, the environmental parameters are now calculated thanks to the acquisition skill of the environmental sensor DHT11. In particular, the function in Fig. 16 has been used to acquire  $t_a$  and RH. At this point of the procedure, the last phase is performed in task 4 (Fig. 24): a supervised ML algorithm has been used to obtain the predicted TSV starting from the data that have been acquired in the previous steps. Specifically, the ML algorithm has been chosen accordingly to literature where SVM,

RF, Decision Trees, Naïve Bayes, and other classifiers have been widely used. As it is possible to appreciate from Fig. 28, a machine learning model is imported (i.e., RF classifier).

```

###TSV prediction
import pickle

my_param = [meantemp, features[0], features[8], hum_fin, temp_fin]
my_param = np.array(my_param).reshape(1,-1)

pickled_model = pickle.load(open('FINAL_TESTmy_pickle', 'rb'))
my_tsv = pickled_model.predict(my_param)
my_tsv_round = round(my_tsv[0], 0)

if my_tsv_round == 0:
    API_ENDPOINT = 'http://' + ip_misty + '/api/images/display?fileName=e_Joy.jpg&alpha=1&layer=DefaultImageLayer&isURL=false'
    r = requests.post(url = API_ENDPOINT)

elif my_tsv_round >= 1:
    API_ENDPOINT = 'http://' + ip_misty + '/api/images/display?fileName=e_Fear.jpg&alpha=1&layer=DefaultImageLayer&isURL=false'
    r = requests.post(url = API_ENDPOINT)

elif my_tsv_round <= -1:
    API_ENDPOINT = 'http://' + ip_misty + '/api/images/display?fileName=e_Terror.jpg&alpha=1&layer=DefaultImageLayer&isURL=false'
    r = requests.post(url = API_ENDPOINT)

dict_finale = {'hrv_raw': hrv, 'hr_raw': hr, 'hrv_features': features,
               't_skin': meantemp, 'ir_frame': frame_in, 'ir_finale': frame,
               'ta': temp_fin, 'rh': hum_fin,
               'tsv_misu': my_tsv, 'tsv_round': my_tsv_round, 'start': time_in, 'end': time_fin }

a_file = open('DATI_PROVE/' + nome_utente + '.pkl', "wb")
pickle.dump(dict_finale, a_file)
a_file.close()

```

**Figure 28.** Python code extract where the ML algorithm is imported for the TSV prediction.

Specifically, the classifier is already trained on a dataset collected during another experimental campaign. Moreover, the input data of the RF are the environmental parameters, the skin temperature of the subject’s forehead, and the HRV features mentioned before. The outcome of the prediction is sent to Misty II via HTTP get requests to obtain a visual output that the participant can immediately appreciate. This outcome is a change in Misty expression that can be observed on the robot display (Fig. 29). In this way, the subject knows his/her comfort conditions and he/she can change the thermal conditions of the room accordingly, improving his/her experience. Indeed:

- the *Joy* expression (Fig. 29 a) comes out if the subject is in comfort (TSV = 0);
- The *Terror* expression (Fig. 29 b) in case of cold discomfort (TSV ≤ −1);
- The *Fear* expression (Fig. 29 c) is the output for the hot discomfort (TSV ≥ 1).



**Figure 29.** The three expressions that can be visualized on Misty II display according to the predicted TSV value. (a) Joy expression for thermal comfort case; (b) Terror expression for cold discomfort case; (c) Fear expression for hot discomfort case.

### 3.4.2 Data processing

The next step of the data analysis procedure consists of the prediction of TSV in post-processing. In fact, the data acquired during the tests are now analysed and processed to achieve a prediction of the subjects' thermal sensation. Once again, Machine Learning is exploited but, in this case, several ML algorithms have been used to compare their predictive power. According to that, it is possible to appreciate in Fig. 30 the block scheme that resumes all the steps that have been implemented to achieve TSV prediction. It can be observed that after the data collection, the acquired parameters have been processed to obtain reliable input data for the ML algorithms. Specifically, this processing phase is focused on the data collected by the smartwatch and the infrared images captured by the low-cost sensor Lepton 3.5.

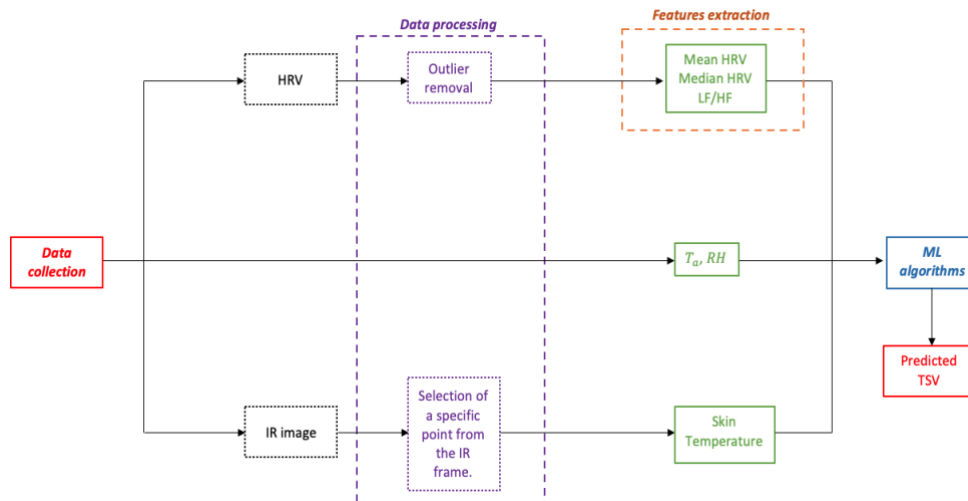


**Figure 30.** Block scheme that resumes all the passages of the second part of data analysis.

Indeed, HR and HRV signals are processed to filter out any value that does not have a physiological meaning. For this reason, the outlier removal process has been implemented. Specifically, every value that was outside the range  $mean \pm 2 * standard\ deviation$  has been deleted and the python library *Hampel* has been used to obtain the final cleaned signal. In Fig. 31, an example of HRV signal and HR signal before and after the outlier removal can be observed. After this step, the HRV feature extraction has been carried out.

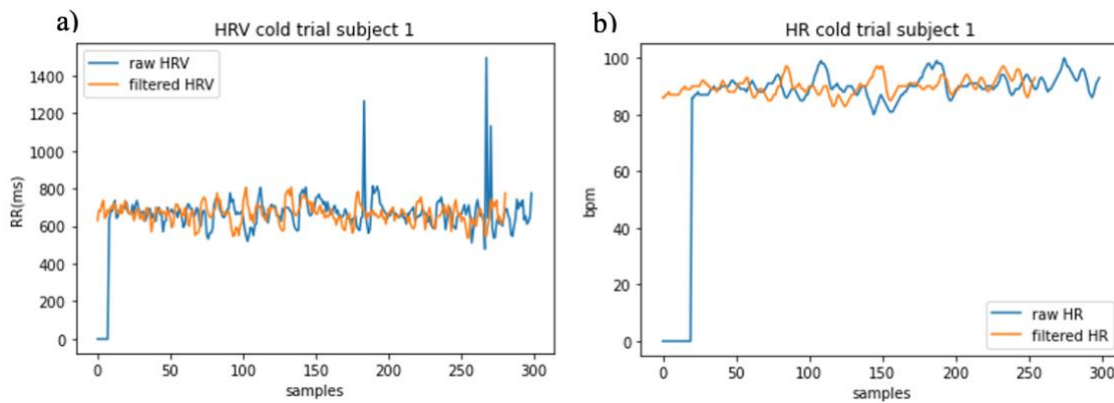


**Figure 31.** (a) HRV signal of subject 1 during the cold trial. (b) the HR signal of subject 1 during the cold trial. In both (a) and (b) the blue trace is the original signal, while the orange one is the processed one.

The time-domain features, mean HRV, and median of HRV have been computed together with the frequency-domain parameter LF/HF, i.e. the ratio between the low frequency (LF) and high frequency (HF) content of the HRV Power Spectral Density (PSD). Several studies have shown that it can be used as a thermal comfort estimation index since it reflects the thermoregulation of a person in an environment.

As regards the processing of the IR sensor output, a python code has been dedicated to the computation of the subjects' skin temperature starting from the selection of a specific point of the IR frame (subjects' forehead, for the current study). Hence, both the coordinates of the point of interest and the corresponding temperature are obtained as output.

Data processing has not been applied to the environmental parameters detected by the sensor DHT11. The reliability of its measurement is tested through the usage of the additional standard instrumentation mentioned before (Fig. 22). Specifically, the data collected by the microclimatic station and the temperature sensor iButton have been considered.

These steps have been crucial for the creation of a suitable dataset for the TSV prediction via different ML algorithms. Indeed, differently from the approach exploited for the real-time TSV prediction a selection of ML procedures has been used accordingly to what the literature states.

**Table 8.** List of the Machine Learning algorithms used in this study.

| <i>Dataset</i>   | <i>Label</i> |
|------------------|--------------|
| Mean HRV         | TSV          |
| Median HRV       |              |
| LF/HF            |              |
| Skin Temperature |              |
| $t_a$            |              |
| $RH$             |              |

**Table 9.** Input dataset for the Machine Learning algorithms used in this study.

| <i>Machine Learning algorithms</i> |
|------------------------------------|
| Random Forest (RF)                 |
| Support Vector Machine (SVM)       |
| Decision Tree (DT)                 |
| Naïve Bayes (NB)                   |
| K-nearest neighbour (KNN)          |
| Bagged Tree (BAG)                  |
| Boosting (ADA)                     |

In Tab. 7 a list of the classifiers used in this study is reported. They have been selected based on literature research [8], [10], [16]. The dataset in Tab. 8 has been divided into two portions: the 80% of the data has been used for the training session of the algorithms, while the 20% of them has been employed for the testing process. Indeed, now the aim is to predict TSV with supervised ML algorithms that have not been already prepared for a prediction. Hence, firstly, these values have been randomized so that the algorithms can recognize the most general pattern of input data. Then, they have been divided as mentioned before. This operation is performed in order to verify if the chosen processes correctly forecast TSV starting from the testing data. All the algorithms have been computed in Python since there is the *sklearn* library that includes several functions for machine learning applications. The choice of computing several ML classifiers aims also at comparing their accuracies to analyse their predictive power and to verify which is the best one for thermal comfort assessment starting from the dataset in Tab. 8. In order to accomplish this task, the python function *accuracy\_score* from the above mentioned

library has been implemented. It mathematically performs the ratio of the sum of true positives and true negatives out of all the predictions (Eq. 4).

$$accuracy = \frac{TP + TN}{TP + FP + TN + FN} \quad (4)$$

TP = True Positive, FP= False Positive, TN = true negative, FN = False Negative

# CHAPTER 4: RESULTS

This chapter reports the outcomes of the present work, discussing also the advantages and disadvantages of the methodology employed for the real-time thermal comfort assessment and the prediction of TSV using ML algorithms.

## 4.1 Feasibility of the robot-based method

The first result of this master thesis is the methodology developed through the integration of all the hardware components described in section 3.1 and all the software logic at the base of the whole procedure (section 3.4.1). Specifically, the proposed method has been tested with the experimental protocol mentioned in section 3.3 and some advantages and disadvantages have been carried out as reported in Tab. 9.

**Table 10.** Pros and Cons of the methodology developed in this master thesis.

| <i>Advantages</i>  | <i>Disadvantages</i>   |
|--|--|
| ⇒ Real-time thermal comfort measurement  | ⇒ The participant has to maintain always the same position during all the trials |
| ⇒ Physiological parameters are included in the thermal comfort measurement (skin temperature, HRV, HR) | ⇒ Uncertainty of wearable sensors with respect to the goal standard (Smartwatch) |
| ⇒ Low-cost and minimally invasive sensors are used   | ⇒ Too short acquisition period (5 minutes).                                      |
| ⇒ The occupant directly interfaces the robot   |  |
| ⇒ User-centered methodology  |  |

## 4.1 Results of TSV prediction in post-processing

Figure 32 encloses the 7 outputs of the TSV predictions performed by the ML algorithms (Tab. 7) starting from the dataset collected during the measurement campaign described in section 3.3. Specifically, the plots in Fig. 32 represent the relationship between the real TSV which has been measured from the 10 participants during the tests, and the TSV predicted by the algorithms. It is clear how some of the employed algorithms succeeded in guessing and estimating the thermal sensation of the subject (RF, NB, DT), while some of them have completely gone wrong with the prediction (SVM, BAG). This is also demonstrated by the accuracies reported in Tab. 10.

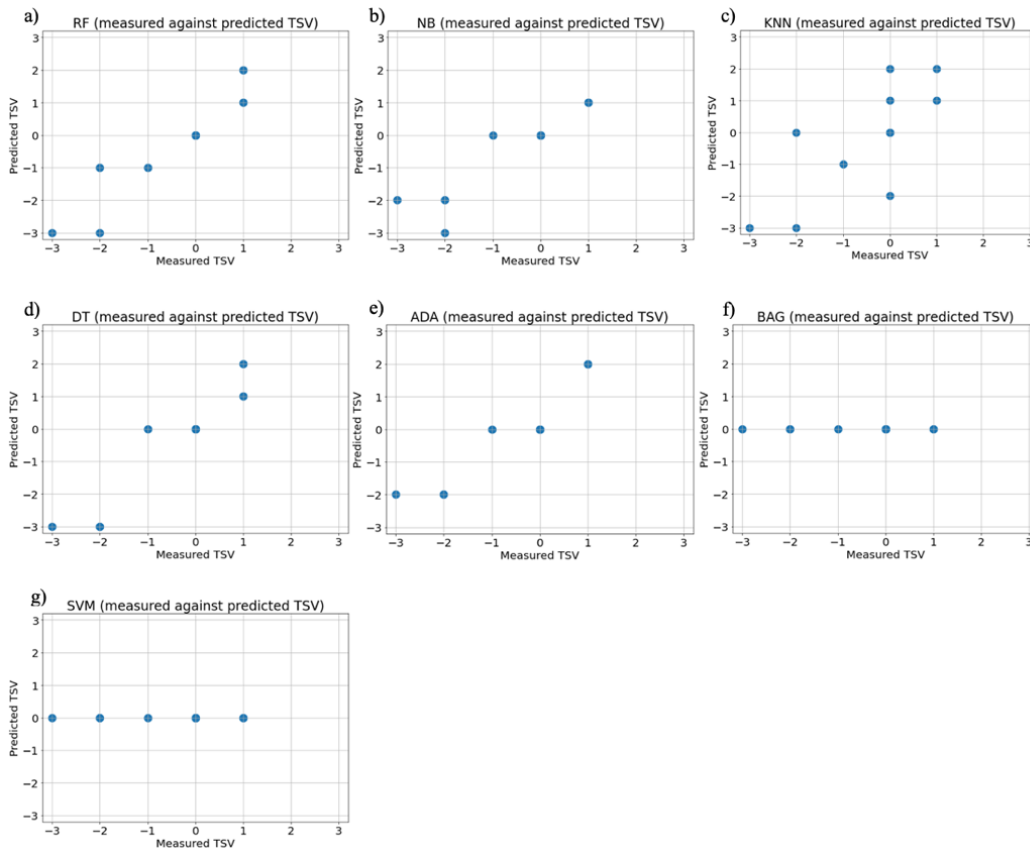


**Figure 33.** Plots of the TSV prediction output against the TSV acquired during the three days of tests from the 10 participants. (a) Plot with Random Forest prediction output. (b) Plot with Naïve Bayes prediction output. (c) Plot with K-Nearest Neighbor prediction output. (d) Plot with Decision Tree prediction output. (e) Plot with Adaboost prediction output. (f) Plot with Bagged Tree prediction output. (g) Plot with Support Vector Machine prediction output.

**Table 11.** Accuracies of the employed ML algorithms.

| <i>ML ALGORITHMS</i>         | <i>ACCURACY (%)</i> |
|------------------------------|---------------------|
| Random Forest (RF)           | 75%                 |
| Support Vector Machine (SVM) | 50%                 |
| Decision Tree (DT)           | 66.67%              |
| Naïve Bayes (NB)             | 75%                 |
| K-nearest neighbor (KNN)     | 50%                 |
| Bagged Tree (BAG)            | 50%                 |
| Boosting (ADA)               | 66.67%              |

## CHAPTER 5: DISCUSSION

In this section, the main points that emerged from the results are presented. Thermal comfort measurement is provided using an innovative human-centric approach that includes a robot with integrated sensors. This goal is achieved with the development of a methodology that exploits the issues and limitations of the state of art as the starting point of an innovative user-centered thermal comfort assessment technique. Traditional approaches (PMV and PPD) give an estimation of thermal comfort that are not always accurate since they refer to a group of subjects and not the single occupant, not considering the intrasubject variability of thermal sensation. The adaptive methods give new importance to the human being inside the building but the employed instrumentations are too invasive and expensive. Moreover, from a computational point of view, the accuracies and efficiency of the process still limit the quality of the assessment. For this reason, machine learning and robotic structures have been introduced in this engineering field. Nevertheless, the most recent studies have used them to detect mainly environmental parameters without giving importance to the user and his/her wellbeing. Based on all these considerations, the current work proposes a methodology that aims at overcoming the above-mentioned limitations gaining higher accuracy in the measurement and enhancing the relevance of the occupant as an active element of the system.

One of the advantages provided by this master thesis is the methodology through which thermal comfort is measured. The occupant is the core of the whole process and a sensors' system simultaneously collects physiological and environmental signals and infrared imaging also exploiting a robotic system. The introduction of the robot Misty II stresses the concept of user-centered method since the employment of a social companion allows the occupant to directly interface with the problem and consequently adjust the surrounding environment accordingly to what the robotic structure measures. Moreover, Misty II can localize itself and move independently with confidence thanks to its onboard sensors. Hence, among all the advantages of Misty II, there is also the possibility to obtain a movable system that can acquire the desired parameters from the integrated IR and environmental sensors.

Finally, the minimally invasive measurement set-up and the low-cost of the equipment are two additional features that should be taken into account.

In section 4.1, Tab. 9 reports all the pros and cons of the proposed method. It is possible to state that all the limitations that the state of art presented concerning thermal comfort assessment are overcome. The robot-based method developed in this master thesis ensures a real-time assessment of thermal comfort considering human health as the main target. In fact, the quantification of thermal comfort starts from the acquisition of the physiological parameters. The user is the focus of the whole process, and he/she is the one that directly interfaces Misty II as described in previous sections (Tab. 9). This allows the occupant to appreciate a real-time output concerning his/her thermal state from the robot and consequently, in a real-life context, the subject can change the thermal condition of the environment. This point of view suggests an improvement of the already present adaptive methods. In fact, the human being is considered an active part of the building as in the adaptive approach, but the difference is that the acquisition gives more importance to physiological parameters and the employed devices are minimally invasive and not expensive.

However, it is also useful to highlight some limitations. For instance, the developed methodology has been tested in a condition that is still not reproducible in real-life contexts because the subject has been asked to always maintain the same position while data are acquired, to facilitate the detection of the face and the subsequent skin temperature measurement from the IR image. In addition, the wearable sensor used in this study is characterized by higher measurement uncertainty of the HRV, if compared with the gold standard (Tab. 9).

## CHAPTER 6: CONCLUSIONS

In the current master thesis, a personalized robot-based method for thermal comfort assessment is designed. It quantifies subjective thermal sensation via physiological signals, infrared imaging, and environmental parameters. This system is minimally invasive and guarantees accurate measurements without adding further instrumentation in the environment. This aspect enhances the relevance of the low-cost and wearable sensors used in this study which may replace standard, but expensive tools. From a technical point of view, the designed robotic architecture is an IoT solution that needs only an internet connection to compute the measurement procedure. This aspect has been highlighted through the developed measurement campaign that involved 10 participants. The data collected during these trials constituted the proper dataset for the seven employed ML algorithms, that have predicted TSV with different accuracies. Among them, the RF classifier and the NB algorithm provided the highest accuracy (75%) (Tab. 10).

Nevertheless, some limitations could be underlined: first of all, ML algorithms are characterized by low accuracies compared to literature examples [8]. Future studies can use a larger input dataset to improve the predictive power of the algorithms. Moreover, the suggested procedure should be tailored for real-life contexts: for instance, if the robot interfaces a worker that does not wear a smartwatch, the prediction of TSV should be implemented anyway without blocking the whole acquisition. Hence, another aspect to analyze in further research is how the robotic structure predicts TSV when not all the devices provide accurate measurement.

Based on these considerations, the current work may pave the way to further improvements and future methodologies which would stress the crucial role of human beings and robotic systems in the thermal comfort scenario.

## REFERENCES

- [1] T. Chaudhuri, Y. C. Soh, H. Li, and L. Xie, “Machine learning driven personal comfort prediction by wearable sensing of pulse rate and skin temperature,” *Build. Environ.*, vol. 170, no. June 2019, p. 106615, 2020, doi: 10.1016/j.buildenv.2019.106615.
- [2] “ASHRAE Transactions,” *ASHRAE Transactions*, vol. 124. p. 152, 2018.
- [3] F. O. R. Standardization and D. E. Normalisation, “International Standard Iso,” vol. 1987, 1987.
- [4] Y. H. Yau and B. T. Chew, “A review on predicted mean vote and adaptive thermal comfort models,” *Build. Serv. Eng. Res. Technol.*, vol. 35, no. 1, pp. 23–35, 2014, doi: 10.1177/0143624412465200.
- [5] N. Morresi *et al.*, “Sensing physiological and environmental quantities to measure human thermal comfort through machine learning techniques,” *IEEE Sens. J.*, vol. 21, no. 10, pp. 12322–12337, 2021, doi: 10.1109/JSEN.2021.3064707.
- [6] B. Yang *et al.*, “Non-invasive (non-contact) measurements of human thermal physiology signals and thermal comfort/discomfort poses -A review,” *Energy Build.*, vol. 224, p. 110261, 2020, doi: 10.1016/j.enbuild.2020.110261.
- [7] D. Li, C. C. Menassa, and V. R. Kamat, “Non-intrusive interpretation of human thermal comfort through analysis of facial infrared thermography,” *Energy Build.*, vol. 176, pp. 246–261, 2018, doi: 10.1016/j.enbuild.2018.07.025.
- [8] A. Aryal and B. Becerik-Gerber, “Thermal comfort modeling when personalized comfort systems are in use: Comparison of sensing and learning methods,” *Build. Environ.*, vol. 185, no. July, p. 107316, 2020, doi: 10.1016/j.buildenv.2020.107316.
- [9] J. Miura, M. Demura, K. Nishi, and S. Oishi, “Thermal comfort measurement using thermal-depth images for robotic monitoring,” *Pattern Recognit. Lett.*, vol. 137, pp. 108–113, 2020, doi: 10.1016/j.patrec.2019.02.014.
- [10] L. Xiong and Y. Yao, “Study on an adaptive thermal comfort model with K-

- nearest-neighbors (KNN) algorithm,” *Build. Environ.*, vol. 202, no. May, p. 108026, 2021, doi: 10.1016/j.buildenv.2021.108026.
- [11] B. Quintana, K. Vikhorev, and A. Adán, “Workplace occupant comfort monitoring with a multi-sensory and portable autonomous robot,” *Build. Environ.*, vol. 205, no. June, 2021, doi: 10.1016/j.buildenv.2021.108194.
- [12] Q. Chai, H. Wang, Y. Zhai, and L. Yang, “Using machine learning algorithms to predict occupants’ thermal comfort in naturally ventilated residential buildings,” *Energy Build.*, vol. 217, p. 109937, 2020, doi: 10.1016/j.enbuild.2020.109937.
- [13] N. Djongyang, R. Tchinda, and D. Njomo, “Thermal comfort: A review paper,” *Renew. Sustain. Energy Rev.*, vol. 14, no. 9, pp. 2626–2640, 2010, doi: 10.1016/j.rser.2010.07.040.
- [14] D. Li, C. C. Menassa, and V. R. Kamat, “Robust non-intrusive interpretation of occupant thermal comfort in built environments with low-cost networked thermal cameras,” *Appl. Energy*, vol. 251, no. March, 2019, doi: 10.1016/j.apenergy.2019.113336.
- [15] O. Kaynakli and M. Kilic, “Investigation of indoor thermal comfort under transient conditions,” *Build. Environ.*, vol. 40, no. 2, pp. 165–174, 2005, doi: 10.1016/j.buildenv.2004.05.010.
- [16] T. Chaudhuri, D. Zhai, Y. C. Soh, H. Li, L. Xie, and X. Ou, “Convolutional Neural Network and Kernel Methods for Occupant Thermal State Detection using Wearable Technology,” *Proc. Int. Jt. Conf. Neural Networks*, vol. 2018-July, 2018, doi: 10.1109/IJCNN.2018.8489069.
- [17] N. Jain *et al.*, “Building performance evaluation of a new hospital building in the uk: Balancing indoor environmental quality and energy performance,” *Atmosphere (Basel)*, vol. 12, no. 1, 2021, doi: 10.3390/ATMOS12010115.
- [18] D. Ormandy and V. Ezratty, “Thermal discomfort and health: protecting the susceptible from excess cold and excess heat in housing,” *Adv. Build. Energy Res.*, vol. 10, no. 1, pp. 84–98, 2016, doi: 10.1080/17512549.2015.1014845.
- [19] S. Tham, R. Thompson, O. Landeg, K. A. Murray, and T. Waite, “Indoor

- temperature and health: a global systematic review,” *Public Health*, vol. 179, pp. 9–17, 2020, doi: 10.1016/j.puhe.2019.09.005.
- [20] A. Ghahramani, G. Castro, B. Becerik-Gerber, and X. Yu, “Infrared thermography of human face for monitoring thermoregulation performance and estimating personal thermal comfort,” *Build. Environ.*, vol. 109, pp. 1–11, 2016, doi: 10.1016/j.buildenv.2016.09.005.
- [21] Y. Yao, Z. Lian, W. Liu, and Q. Shen, “Experimental study on skin temperature and thermal comfort of the human body in a recumbent posture under uniform thermal environments,” *Indoor Built Environ.*, vol. 16, no. 6, pp. 505–518, 2007, doi: 10.1177/1420326X07084291.
- [22] Y. Yao, Z. Lian, W. Liu, C. Jiang, Y. Liu, and H. Lu, “Heart rate variation and electroencephalograph - The potential physiological factors for thermal comfort study,” *Indoor Air*, vol. 19, no. 2, pp. 93–101, 2009, doi: 10.1111/j.1600-0668.2008.00565.x.
- [23] J. R. Lim, G. H. Baek, and E. S. Jeon, “Analysis of the Correlation between Thermal Sensations and Brain Waves via EEG Measurements,” *Int. J. Appl. Eng. Res.*, vol. 13, no. 8, pp. 6069–6075, 2018.
- [24] D. Li, C. C. Menassa, and V. R. Kamat, “Personalized human comfort in indoor building environments under diverse conditioning modes,” *Build. Environ.*, vol. 126, no. October, pp. 304–317, 2017, doi: 10.1016/j.buildenv.2017.10.004.
- [25] W. Liu, Z. Lian, and Y. Liu, “Heart rate variability at different thermal comfort levels,” *Eur. J. Appl. Physiol.*, vol. 103, no. 3, pp. 361–366, 2008, doi: 10.1007/s00421-008-0718-6.
- [26] I. Nastase, C. Croitoru, and C. Lungu, “A Questioning of the Thermal Sensation Vote Index Based on Questionnaire Survey for Real Working Environments,” *Energy Procedia*, vol. 85, no. November 2015, pp. 366–374, 2016, doi: 10.1016/j.egypro.2015.12.263.
- [27] E. E. Broday, J. A. Moreto, A. A. de P. Xavier, and R. de Oliveira, “The approximation between thermal sensation votes (TSV) and predicted mean vote (PMV): A comparative analysis,” *Int. J. Ind. Ergon.*, vol. 69, no. October 2018,

- pp. 1–8, 2019, doi: 10.1016/j.ergon.2018.09.007.
- [28] D. Markov, “Practical evaluation of the thermal comfort parameters,” *Annu. Int. Course Vent. Indoor Clim. Avangard, Sofia*, no. October 2002, pp. 158–170, 2002.
- [29] A. Pourshaghaghay and M. Omidvari, “Examination of thermal comfort in a hospital using PMV-PPD model,” *Appl. Ergon.*, vol. 43, no. 6, pp. 1089–1095, 2012, doi: 10.1016/j.apergo.2012.03.010.
- [30] E. Arens, M. A. Humphreys, R. de Dear, and H. Zhang, “Are ‘class A’ temperature requirements realistic or desirable?,” *Build. Environ.*, vol. 45, no. 1, pp. 4–10, 2010, doi: 10.1016/j.buildenv.2009.03.014.
- [31] A. Satake, H. Ikegami, and Y. Mitani, “Energy-saving Operation and Optimization of Thermal Comfort in Thermal Radiative Cooling/Heating System,” *Energy Procedia*, vol. 100, no. September, pp. 452–458, 2016, doi: 10.1016/j.egypro.2016.10.201.
- [32] R. Becker and M. Paciuk, “Thermal comfort in residential buildings - Failure to predict by Standard model,” *Build. Environ.*, vol. 44, no. 5, pp. 948–960, 2009, doi: 10.1016/j.buildenv.2008.06.011.
- [33] S. Lu, W. Wang, S. Wang, and E. C. Hameen, “Thermal comfort-based personalized models with non-intrusive sensing technique in office buildings,” *Appl. Sci.*, vol. 9, no. 9, 2019, doi: 10.3390/app9091768.
- [34] E. Halawa and J. Van Hoof, “The adaptive approach to thermal comfort: A critical overview,” *Energy Build.*, vol. 51, pp. 101–110, 2012, doi: 10.1016/j.enbuild.2012.04.011.
- [35] R. F. Ribeiro, M. Fernandes, and J. R. Neves, “Face Detection on Infrared Thermal Image,” *Signal 2017*, no. March 2019, pp. 38–42, 2017.
- [36] A. Aryal and B. Becerik-Gerber, “Skin temperature extraction using facial landmark detection and thermal imaging for comfort assessment,” *BuildSys 2019 - Proc. 6th ACM Int. Conf. Syst. Energy-Efficient Build. Cities, Transp.*, pp. 71–80, 2019, doi: 10.1145/3360322.3360848.
- [37] J. Kim, S. Schiavon, and G. Brager, “Personal comfort models – A new paradigm

- in thermal comfort for occupant-centric environmental control,” *Build. Environ.*, vol. 132, no. January, pp. 114–124, 2018, doi: 10.1016/j.buildenv.2018.01.023.
- [38] K. N. Nkurikiyeyezu, Y. Suzuki, and G. F. Lopez, “Heart rate variability as a predictive biomarker of thermal comfort,” *J. Ambient Intell. Humaniz. Comput.*, vol. 9, no. 5, pp. 1465–1477, 2018, doi: 10.1007/s12652-017-0567-4.
- [39] M. Jin, S. Liu, S. Schiavon, and C. Spanos, “Automated mobile sensing: Towards high-granularity agile indoor environmental quality monitoring,” *Build. Environ.*, vol. 127, no. October 2017, pp. 268–276, 2018, doi: 10.1016/j.buildenv.2017.11.003.
- [40] M. Surya, D. Gupta, V. Patchava, and V. Irginia Menezes, “Healthcare based on IoT using Raspberry Pi,” no. 1, pp. 1–4.
- [41] N. Morresi, S. Casaccia, M. Sorcinelli, M. Arnesano, and G. M. Revel, “Analysing performances of Heart Rate Variability measurement through a smartwatch,” *IEEE Med. Meas. Appl. MeMeA 2020 - Conf. Proc.*, 2020, doi: 10.1109/MeMeA49120.2020.9137211.
- [42] B. M. Charvát, “BRNO UNIVERSITY OF TECHNOLOGY SYSTEM FOR PEOPLE DETECTION AND LOCALIZATION USING THERMAL IMAGING CAMERAS Master ’ s Thesis Specification,” 2020.
- [43] A. Valeriano and D. G. N. S. Order, “INTERNATIONAL STANDARD Energy performance of buildings — Indoor environmental quality — parameters for the design and,” vol. 2017, 2017.